Analytica Chimica Acta 803 (2013) 15–40

Contents lists available at ScienceDirect

Analytica Chimica Acta

journal homepage: www.elsevier.com/locate/aca

Review

Flow injection analysis as a tool for enhancing oceanographic nutrient measurements—A review

Paul J. Worsfold[a], Robert Clough[a], Maeve C. Lohan[a], Philippe Monbet[b], Peter S. Ellis[c], Christophe R. Quétel[d], Geerke H. Floor[d], Ian D. McKelvie[a,e,*]

[a] School of Geography, Earth and Environmental Sciences, Plymouth University, Plymouth, PL4 8AA, United Kingdom
[b] Pole Mer Bretagne, CS 83809, 29238 Brest Cedex 3, France
[c] Water Studies Centre, School of Chemistry, Monash University, Clayton, 3800, Australia
[d] Institute for Reference Materials and Measurements, Joint Research Centre – European Commission, 111 Retieseweg, B-2440 Geel, Belgium
[e] School of Chemistry, The University of Melbourne, Parkville, 3010, Australia

HIGHLIGHTS

- FIA and SIA techniques for nutrient determinations in marine waters are critically reviewed.
- The advantages and suitability of FIA for underway and shipboard marine analysis are discussed.
- Strategies for sensitivity improvement are considered.
- Potential schlieren problems in FIA of marine samples and possible solutions proposed.
- The importance of data quality and uncertainty estimation in trace analysis are emphasised.

GRAPHICAL ABSTRACT

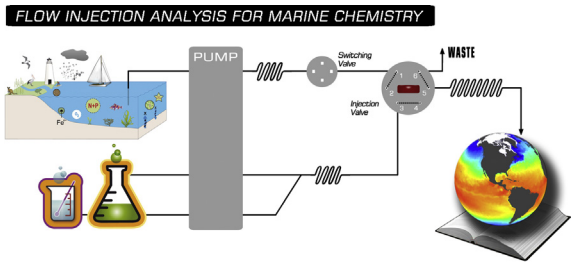

ARTICLE INFO

Article history:
Received 27 April 2013
Received in revised form 13 June 2013
Accepted 15 June 2013
Available online 20 June 2013

Keywords:
Marine waters
Estuarine waters
Macronutrients

ABSTRACT

Macronutrient elements (C, N and P) and micronutrient elements (Fe, Co, Cu, Zn and Mn) are widely measured in their various physico-chemical forms in open ocean, shelf sea, coastal and estuarine waters. These measurements help to elucidate the biogeochemical cycling of these elements in marine waters and highlight the ecological and socio-economic importance of the oceans. Due to the dynamic nature of marine waters in terms of chemical, biological and physical processes, it is advantageous to make these measurements in situ and in this regard flow injection analysis (FIA) provides a suitable shipboard platform. This review, therefore, discusses the role of FIA in the determination of macro- and micro-nutrient elements, with an emphasis on manifold design and detection strategies for the reliable shipboard determination of specific nutrient species. The application of various FIA manifolds to oceanographic nutrient

Abbreviations: 8HQ-MAF, 8-quinolinol immobilised on silica gel, metal alkoxide fluoride glass; C4 D, contactless capacitively coupled conductivity detector; CL, chemiluminescence; CRM, certified reference material; CTAB, cetyltrimethylammonium bromide; DIC, dissolved inorganic carbon; DDAB, didodecyldimethylammonium bromide; DIC, dissolved inorganic carbon (also called "total carbonate"); DOC, dissolved organic carbon; DOP, dissolved organic phosphorus; DRP, dissolved reactive phosphorus; FIA, flow injection analysis; GD, gas diffusion; GF-AAS, graphite furnace atomic absorption spectrophotometry; GUM, guide to the expression of uncertainty in measurements; HNLC, high-nutrient, low-chlorophyll regions; HTCO, high temperature catalytic oxidation; ICP-SFMS, inductively coupled plasmas-sector field mass spectrometry; id, inside diameter; ID, isotope dilution; IDA, iminodiacetate resin; LOC, Lab-on-Chip; LOD, limit of detection; LWCC, liquid waveguide capillary cell; MRFC, multi-reflection flow cell; NOx, nitrate + nitrite; NTA, nitriloacetic acid; od, outside diameter; OPA, orthophthaldialdehyde; p_{CO_2}, partial pressure of carbon dioxide; PON, particulate organic nitrogen; PSII, Photosystem II; RI, refractive index; RM, reference material; ROV, remotely operated vehicle; RSD, relative standard deviation; REU, relative expanded uncertainty; S, salinity; SAFe, sampling and analysis of iron program; SCFA, segmented continuous flow analysis; SOD, superoxide dismutase; SP, spectrophotometry; $\sum CO_2$, dissolved inorganic carbon (also called "total carbonate"); TA, total alkalinity; TC, total carbon; TCNQ, 7,7,8,8-tetracyanoquinodimethane; T_{CO_2}, dissolved inorganic carbon (also called "total carbonate"); TDN, total dissolved nitrogen; TDP, total dissolved phosphorus; TIC, total inorganic carbon; TOC, total organic carbon; TN, total nitrogen; TP, total phosphorus; TPN, total particulate nitrogen.

* Corresponding author.
E-mail address: ian.mckelvie@gmx.com (I.D. McKelvie).

0003-2670/$ – see front matter
http://dx.doi.org/10.1016/j.aca.2013.06.015

Micronutrients
Flow injection analysis
Data quality

determinations is discussed, with an emphasis on sensitivity, selectivity, high throughput analysis and suitability for underway analysis and depth profiles. Strategies for enhancing sensitivity and minimizing matrix effects, e.g. refractive index (schlieren) effects and the important role of uncertainty budgets in underpinning method validation and data quality are discussed in some detail.

Contents

Paul J. Worsfold is a Professor of Analytical Chemistry at Plymouth University (since 1990) and Co-Director of the Biogeochemistry Research Centre. He obtained his BSc from Loughborough University (1976) and his PhD from the University of Toronto (1980). He is Chair of the Division of Analytical Chemistry of the European Association for Chemical and Molecular Sciences and a Past-President of the Analytical Division of the Royal Society of Chemistry. One research interest is techniques for the determination of macronutrients and micronutrients and understanding their role in terrestrial and aquatic biogeochemical processes. Flow injection provides an integrating theme for this research and he has recently co-authored a textbook on the subject.

Robert Clough has been a research fellow in the School of Geography, Earth and Environmental Sciences at the University of Plymouth since 2003 having also obtained his BSc and PhD at Plymouth. He is currently Chair of the Western region of the Analytical Division of the Royal Society of Chemistry and a Topic Group co-ordinator for the Atomic Spectrometry Updates annual reviews. Robert's research interests focus on elemental speciation, analytical method development and chemical metrology, applying this to difficult to measure analytes in challenging sample matrices.

Maeve C. Lohan is a Professor in marine chemistry at the University of Plymouth. Her research interests focus on understanding trace metal biogeochemical cycling in both coastal and open ocean regimes with particular reference to bioactive metals such as iron, zinc, and cobalt. In particular, her research focuses on the speciation of these elements and their bioavailability and impact on aquatic ecosystems.

Philippe Monbet With a background in chemistry obtained from the University of Western Brittany, Philippe Monbet completed a PhD in "Marine Chemistry and Analytical Chemistry" at the European Institute for Marine Studies (IUEM, Brest) on the dynamics heavy metals in an estuary subject to strong agricultural inputs. He then joined French research institutes IFREMER and INERIS for missions of research and expertise. His research activities have taken him to AIMS (the Australian Institute of Marine Science, Townsville, Australia), Monash University (Melbourne, Australia) and Plymouth University (UK) where his research was mainly devoted to phosphorus biogeochemistry in coastal ecosystems.

Peter S. Ellis has been a Research Fellow in the Water Studies Centre, Monash University since 1998. With a background in electronics and optics, his recent research has focussed on the development of portable flow based analytical systems for the underway measurement of macronutrients in marine and estuarine systems. His flow systems have been extensively used for coastal marine measurements around Australia and further afield. Of particular interest has been the development of high sensitivity spectrophotometric detection systems with low susceptibility to schlieren errors.

Christophe R. Quétel graduated in 1987 in physical chemistry from the École Nationale Supérieure de Chimie Physique de Bordeaux, France. He completed a PhD thesis in marine chemistry at the Commissariat à l'Energie Atomique (Gif-sur-Yvette, France) and received his diploma from the University Paris VI in 1991. Subsequently, he held post-doctoral fellowships at the University of Bordeaux and at the National Institute for Resources and Environment in Tsukuba, Japan, before moving to the Institute for Reference Materials and Measurements (IRMM) of the Joint Research Centre of the European Commission (Geel, Belgium) in 1996. Here, he established the IRMM ICP-MS laboratory, developing projects on isotopic reference measurements and reference materials, and chemical metrology. He has published more than 75 articles and given more than 60 invited lectures at conferences and workshops. He chaired the Euramet MetChem-Technical Committee for Inorganic Analysis 2004 to 2010 and represents the IRMM on the Inorganic Analysis Working Group of the Comité Consultatif pour la Quantité de Matière. He has been the President of the French Society for Stable Isotopes from 2006 to 2012, and is Joint Editor in Chief of *Geostandards and Geoanalytical Research*.

Geerke H. Floor obtained her MSc from the Department of Earth Sciences, Utrecht University in 2007 and a PhD in Environmental Analytical Chemistry from the Department of Chemistry, University of Girona in 2011. Her research is at the interface between Earth Sciences and Analytical Chemistry. Geerke is working at the Institute for Reference Materials and Measurements (a European Commission Joint Research Centre) since 2011 with a main focus on the development of analytical protocols for environmental applications using the concept of isotope dilution.

Ian D. McKelvie is Principal Fellow in the School of Chemistry at the University of Melbourne and Visiting Professor, School of Geography, Earth, and Environmental Sciences, at the Plymouth University, UK. Prior to that he was Associate Professor at Monash University, where his research focused on the development of flow-based analytical systems for water quality assessment of macronutrients in marine, estuarine and freshwater systems, and on the biogeochemistry of organic phosphates. He has co-edited two monographs: Environmental Monitoring Handbook (2002) and Advances in flow injection analysis and related techniques (2008), and recently joined the journal *Talanta* as an associate editor.

1. Introduction

Macronutrients (C, N and P species) and micronutrients (particularly Fe, Co, Cu, Zn and Mn) are widely measured in open ocean, coastal and estuarine waters. The drivers for these measurements relate to both the ecological and socio-economic importance of the oceans. The oceans are estimated to contribute ca. 21 trillion US$/year to human welfare (cf. a global GNP of ~25 trillion US$). Open ocean contributes ca. 40% of this amount, and coastal and shelf systems are responsible for the remaining 60% [1,2].

The effect of industrialization and population growth in many countries has been to increase the inputs of macronutrients (especially P and N) to estuaries and coastal waters [3] which in many instances has resulted in cultural eutrophication i.e. "the anthropogenic enrichment of the environment with nutrients and the concomitant production of undesirable effects" [4]. While elevated macronutrient concentrations do not inevitably lead to trophic changes in marine systems, they are the principal cause where this occurs. Cultural eutrophication is now occurring in many estuarine and coastal areas of the globe because of continuing population growth, coastal zone urbanisation and industrialisation [5–8]. The numerous undesirable effects resulting from nutrient enrichment [9] include localised high concentrations of suspended algae, harmful algal blooms, extreme dissolved oxygen depletion, and death of biota. The economic costs of these adverse effects are potentially enormous, but are rarely assessed [10]. Climate change is expected to increase the inputs of macronutrients to estuaries, exacerbating eutrophication in coastal waters [11]. Furthermore, the role of nutrients in the oceanic sequestration of atmospheric CO_2 is not thoroughly understood. For example, the subtropical oligotrophic (low nutrient and low biomass) regions of the ocean cover almost 50% of the Earth's surface. These regions, previously thought to be spatially homogenous and unvarying, respond to episodic nutrient inputs with transient pulses of C sequestration [12]. However, measurement of macro- and micro-nutrients in these environments is challenging because of the generally very low concentrations encountered.

Micronutrients are defined by their involvement in marine primary productivity and their vertical profiles in the water column indicate an association with biogenic particles. The lowest concentrations of essential micronutrients, i.e. those directly involved in primary production, are observed in the surface ocean. These elements are taken up by organisms in surface waters and released back into the water column following decomposition in deeper waters or at the sediment–water interface, resulting in vertical oceanic profiles with surface depletion and enrichment at depth.

Speciation, which describes the individual physico-chemical forms of an element, includes free aqueous ions, ion pairs, complexes (both inorganic and organic), colloids and particles. In addition, trace metal micro-nutrients can have different oxidation states in the marine environment, which exhibit differences in availability for uptake by organisms, toxicity and particle reactivity. For example, free aqueous Cu^{2+} ions appear to be the available form for the dinoflagellate *Gonyaulax tamarensis*, with enhanced Cu^{2+} concentrations resulting in toxic effects ($[Cu^{2+}] > 10^{-10.4}$ mol L^{-1}) and low levels resulting in Cu deficiency with reduced growth ($[Cu^{2+}] < 10^{-12.5}$ mol L^{-1}) [13,14].

There are significant analytical challenges in determining micronutrients in the marine environment. Iron, for example, is ubiquitous in the terrestrial environment and yet exhibits low (sub-nM) concentrations in the oceanic environment. Dissolved Fe

concentrations are typically < 0.1 nM in oceanic surface waters with slightly higher concentrations in deeper waters (ca. 0.4–0.8 nM) for stations in the North Atlantic and North Pacific [15,16]. Iron also exhibits strong temporal and spatial variability in marine waters. Factors such as ocean acidification and phytoplankton blooms may also mobilise redox-sensitive trace metals such as iron and autumn storms can erode water column stratification and oxygenate the water, resulting in the removal of redox sensitive metals.

Improved analytical techniques are required for the accurate determination of different micronutrient species in seawater, e.g. in the case of iron, free Fe(II) or Fe(III) ions are thought to be the accessible Fe species for algae, with organic ligands, including bacterial exudates such as siderophores, involved in complexing Fe [14]. The "colloidal" fraction is also thought to be an important fraction of the "dissolved" iron pool in the ocean. As a result of the transient nature of the chemical equilibrium between the various dissolved Fe species, it is important that measurements are performed immediately after sampling. Automated shipboard flow injection based analytical systems can therefore make a significant contribution to high-resolution, contamination-free oceanic Fe speciation measurements.

National and international legislation frameworks and guidelines have been introduced for the protection of vulnerable marine and freshwater environments, e.g. the London [17], Helsinki [18] and Barcelona Conventions [19], and the EU Directives (Habitats [20], and Marine Framework [21]). Evaluation of remediation strategies for nutrient contaminated ecosystems requires that nutrient measurements are undertaken, either in a monitoring context, i.e. mapping of the impacted environment spatially and/or temporally, to examine key nutrient transport and cycling processes, or to assess the bioavailability of nutrient species.

The latter aspect is important, since not all of the physico-chemical forms of nutrient species are biologically available. Consequently, nutrient measurements should differentiate between those fractions or species that may be bioavailable, e.g. dissolved, ionic forms, and the total concentration, which includes less bioavailable particulate, colloidal and organic forms. Hence there is a need for tools that can provide accurate, precise, high quality measurements of nutrient parameters of macro- and micro-nutrients in marine and estuarine waters. Such techniques should be capable of determining specified nutrient forms and total nutrients, often at low concentrations, in waters of varying salinity. They should also be amenable to high sample throughput, enabling the study of spatially and temporally variable systems. Flow analysis techniques offer the potential for on-line sample manipulation and preconcentration, and fulfil all of the requirements listed above.

This review therefore discusses the role of flow injection techniques in the determination of macro- and micro-nutrient species, with a focus on manifold design and detection strategies. The role of uncertainty budgets and other metrological processes in ensuring data quality are emphasized. Applications of these manifolds to oceanographic analysis are discussed with an emphasis on sensitivity, selectivity, high throughput analysis and suitability for underway analysis and depth profiling deployment. Strategies for enhancing sensitivity and minimizing matrix effects, e.g. refractive index (schlieren) effects, are discussed in detail.

2. Flow analysis techniques for nutrient measurement

In flow injection, sequential injection and related techniques, sample is reproducibly injected into carrier or reagent streams that are transported in small diameter conduits (typically 0.5–0.8 mm internal diameter) under *laminar* flow conditions [22]. In this hydrodynamic regime, partial but controlled sample zone dispersion occurs, and there is no need for reactions to reach equilibrium before detection. The consequence of this is that sample and reagent usage is low and sample throughput is generally high. This is in contrast to an older and commonly used technique, viz.; segmented continuous flow analysis (SCFA) which operates under *turbulent* flow conditions with bubble segmentation, with the requirement that detection reactions reach a steady state. Hence flow injection analysis is not merely segmented flow analysis without the bubbles, but a technique that operates under quite different flow conditions that confer a number of additional advantages, such as the ability to perform kinetic measurements using transient signals, on-line preconcentration and column separation methods on-line [23].

There are several identifiable generations of flow injection systems, all of which are currently used to advantage in oceanographic analysis. The first generation of FIA involved the injection of a discrete sample zone into a continuously flowing carrier with continuous merging of one or more reagent streams (Fig. 1). Because the system operates under continuous flow conditions, high sample throughput is possible, but at a cost of higher reagent usage. Flow manifolds also need to be reconfigured for each parameter measured. A variation on conventional flow injection analysis are the so-called reverse flow injection or reagent injection systems where one or more reagents are injected into a continuously pumped stream of sample, thus minimizing reagent consumption [24].

A second generation system, sequential injection analysis, utilizes the principle of multi-commutation and involves the use of a multi-port selection valve and a single reversible pump which enables the sandwiching of sample and reagent zones in an inert carrier stream (Fig. 1). This approach has the advantage of simplifying the instrumentation, and modification of the hydrodynamic conditions can be achieved by simply changing the valve and pump programming.

A third generation system, Lab-on-Valve, is similar in concept to sequential injection, but involves integration of all flow manifold elements and the detector flow cell into a micro-conduit attached to the back of the selection valve.

The advantages of flow and sequential injection techniques include:

- High sample throughput.
- Minimum sample and reagent use.
- High precision measurement.
- Ability to condition samples on-line, e.g. filtration, dialysis, digestion.
- Ability to manipulate samples on-line, e.g. preconcentration, enzymatic hydrolysis, membrane and chromatographic separation.
- Ability to perform determinations based on transient species, e.g. measurements involving chemiluminescence emission from excited state species.
- Highly amenable to on-line measurement, e.g. underway shipboard measurements.

Spatial and temporal data collection at sea is readily achieved by pumping sample directly from the sea, e.g. water for macronutrients can be pumped from the cooling water intake of the vessel to a shipboard flow analysis system. For example, "FerryBox" systems have been used on board commercial European ferries since 2001 for the autonomous, collection of physico-chemical spatial data (temperature, salinity, turbidity, pH, oxygen, chlorophyll-a, some nutrients) [25]. Alternatively seawater samples can be collected via a towed torpedo-shaped "fish", deployed off the crane arm of a hydrographic winch, typically at a distance of ~5 m from the ship, and connected to a deck mounted all-Teflon® diaphragm pump by Teflon®-PVA tubing. In both approaches, sample degassing and filtration can be incorporated in-line and the filtered sample

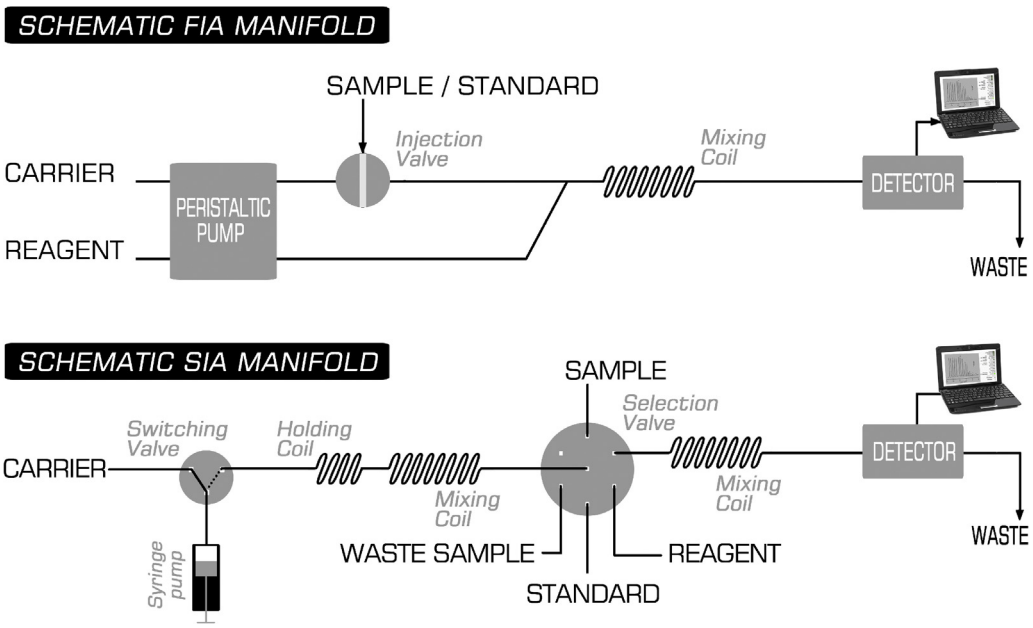

Fig. 1. Schematic diagrams of simple flow injection analysis (FIA) system and sequential injection analysis (SIA) systems.

pumped directly to the flow analysis system and/or collected for off-line analysis. This approach minimises contamination and preconditions the sample, as demonstrated in the chemiluminometric determination of Fe(II) in surface seawater [26]. An alternative sampling approach is to deploy a submersible analyser [27]. Water is drawn from the exterior environment by an on-board pump in order to fill the sampling loop, with excess sample directed back to the exterior. The flow system is remotely controlled and the results can either be stored in the analyser or transmitted back to the ship via a cable. Excellent temporal and spatial resolution can be achieved which is crucial for investigating dynamic processes in estuarine, coastal and open ocean waters [28].

3. High sensitivity detection strategies

3.1. Spectrophotometric detection

Enhancement of sensitivity in spectrophotometric detection can be achieved by manipulating any of the variables absorptivity, ε, optical pathlength, b, or concentration, C in the Lambert–Beer Law. For example, the sensitivity of the spectrophotometric determination of phosphate, most frequently determined as phosphomolybdenum blue ($\varepsilon = 2.27 \times 10^4\ \mathrm{mol^{-1}\,L\,cm^{-1}}$ [29]), can be improved by the formation of the phosphomolybdate–Malchite Green ion pair to give a more strongly absorbing chromophore ($\varepsilon = 7.8 \times 10^4\ \mathrm{mol^{-1}\,L\,cm^{-1}}$ [30]). Alternatively, use of preconcentration techniques, which are discussed in Section 3.3, can be applied so that trace analytes can be detected in even the most pristine of waters.

The third possibility is to increase the optical pathlength, b, of the flow through spectrophotometric detection cell. One way this can be achieved is by the use of a multi-reflection flow cell (MRFC), in which light from the detector source is introduced transversely into a mirror-coated conduit and undergoes multiple reflections before passing through an exit window in the side of the capillary [31,32] (Fig. 2a and b). The number of reflections along the capillary will be a function of the angle of incidence into the capillary, the dimensions and refractive indices of the capillary walls and capillary bore, and the distance between the incident and emergent light windows. The use of thin-walled capillaries coupled with the appropriate incident angle can result in the optical path through the liquid core being somewhat greater than the physical length of the illuminated capillary (Fig. 2a). The use of an uninterrupted capillary flow cell, i.e. without T-piece fluidic connections, is also advantageous because it minimises sample dispersion and stray bubble entrapment. Since the light beam from the detector source enters the capillary almost orthogonal to the direction of flow through the capillary, the schlieren effect (discussed in Section 4) is also minimised, which is an important consideration in the

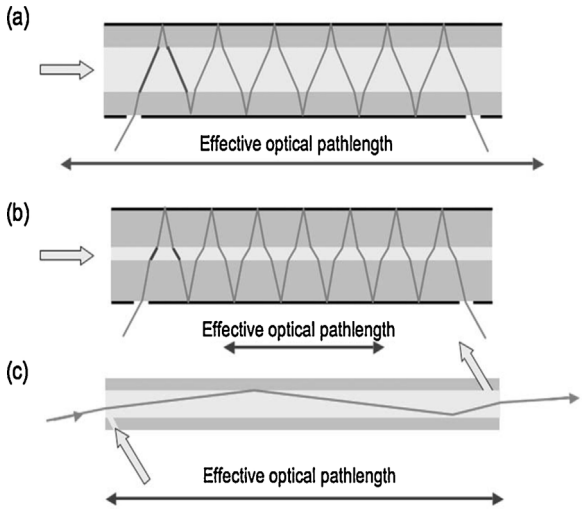

Fig. 2. Simplified representation of the principle of multi-reflection flowcells, showing the importance of the capillary i.d. and wall thickness on the effective optical pathlength. The optical behaviour is complicated in round capillaries by rotary reflection of light, use of non- collimated incident beams and light transmission through the capillary wall. (a) Capillary i.d. > wall thickness: effective optical pathlength > length of the capillary. (b) Capillary i.d. < wall thickness: effective optical pathlength < length of the capillary. The darker segments show the effective pathlength of a single reflection, and the arrow below each diagram represents the sum of all such illuminated segments that comprise the effective optical pathlength. (c) Schematic diagram of the light behaviour in a liquid-core waveguide detection cell which illustrates the similarity between the effective optical pathlength and the length of the capillary. Diagram and caption reproduced from Ref. [40] with permission.

analysis of waters of varying salinity. MRFCs have been used to advantage in a number of estuarine coastal marine studies [33–38].

Increasing the optical pathlength can also be achieved by the use of liquid waveguide capillary cells (LWCC) that consist of either Teflon AF1600® or AF2400® capillaries or silica capillaries externally coated with the same fluoropolymers. Teflon AF1600® or AF2400® have refractive indices of less than water, and if light is introduced at greater than the critical angle into a capillary containing an aqueous liquid, it undergoes total internal reflection, and is propagated along the entire length of the capillary (Fig. 2c). Capillary flow cells, with optical pathlengths of 1 m or more can be used for absorbance measurement, with concomitant increases in absorbance [39]. However, the substantial increase in sensitivity that can be achieved using LWCCs is often accompanied by an increase in the blank value. Since the limit of detection is a also function of the signal-to-noise ratio, the observed improvement in detection limit may be less than that expected based on increased pathlength and sensitivity considerations. LWCCs, because of their long length, will increase sample dispersion and are also be susceptible to entrapment of bubbles and optical scattering by colloidal matter. Schlieren effects can be quite problematic in LWCCs because the critical angle for total internal reflection is such that the light path is close to the axial flow of the liquid core [40]. Despite these limitations, use of LWCCs is one of the easiest and increasingly popular means of improving sensitivity, and their application has been described for the determination of nanomolar concentrations of phosphate [41–43], nitrate [42] and silicate [44].

3.2. Luminescence detection

Fluorescence occurs when analyte molecules absorb light to form short-lived excited state species (the typical lifetime of an excited singlet state in fluorimetry is 10^{-9} to 10^{-6} s). When these excited molecules relax, radiation is emitted that is usually of less energy (longer wavelength) than the energy absorbed because some energy is lost through vibrational relaxation [45,46]. For dilute solutions, the relationship between fluorescence power and analyte concentration is approximated by:

$$F = k''\phi_f P_i \varepsilon b C \quad (1)$$

where F = fluorescence radiant power, k'' = an experimental factor that includes reaction quantum yield, sample dispersion, detector geometry and detector efficiency, $\emptyset_f$ = fluorescence efficiency, P_i = power of incident light beam, ε = molar absorptivity, b = optical pathlength and C = concentration in moles per litre [47].

In designing a flow system for the measurement of analyte fluorescence, consideration must be given to the loss of sensitivity that will occur if the flow rate is too high or the flow cell volume is small and a proportion of the fluorescing sample zone emerges from the flow cell without emitting light, or conversely if the flow rate is too low and a portion of analyte molecules emit fluorescence before reaching the flow cell. Optimisation of this time window is most critical in flow systems where fluorescent emission is slow [47]; the same considerations apply to flow analysis involving detection by chemiluminescence and bioluminescence.

Fluorescence measurement is intrinsically more sensitive than spectrophotometry because it relies principally on the intensity of emitted light with little background signal rather than on the ability to differentiate between incident and transmitted radiation. Consequently fluorescence is a favourable method of detection for some trace species in marine analysis, and flow analysis methods have been reported for phosphate [48,49], ammonia [50], nitrite and nitrate [49] and zinc [51,52].

Chemiluminescence (CL) involves the production of ultraviolet, visible or infrared light by a chemical reaction. Solution phase CL reactions are characterized by high sensitivity and a wide linear dynamic range. The high sensitivity achieved by CL is largely due to the lack of requirement for a radiation source, which minimises Rayleigh and Raman scattering and source noise [53]. Detectors can therefore be operated using high photomultiplier voltages, resulting in a marked improvement in signal-to-noise compared with that experienced in conventional spectrophotometric or fluorimetric detection; femtomole and even attomole detection limits have been reported using CL [47]. This makes CL an attractive means of detection in oceanographic analysis, and its use in this and related areas has been extensively reviewed by Bowie et al. [54] and Robards and Worsfold [55].

Numerous inorganic and organic chemical reactions are known to produce CL, either directly or indirectly (involving the use of a sensitiser or energy transfer agent). Any species whose concentration defines the reaction rate in a chemiluminescent process can be quantified by measuring the intensity of chemiluminescence. In many cases it is possible to manipulate the reaction conditions such that any reaction component, e.g. substrate, oxidant, sensitiser, enzyme cofactor, can be measured as the analyte by adjusting the concentration so that it becomes rate limiting.

The fast and transient nature of solution chemiluminescence reactions requires rapid and reproducible sample and reagent mixing, and FIA provides the ideal means of performing these fluidic manipulations [56,57]. For example, the luminol reaction is commonly used as the basis for the chemiluminescent determination of trace metals and hydrogen peroxide in seawater [58,59]. This involves the oxidation of luminol (5-amino-2,3-dihydrophthalazine-1,4-dione) at pH 9.5–11 with catalysts such as haeme-containing enzymes (e.g. peroxidase) or metal ions such as cobalt(II), copper(II) and iron(II). Due to the rapid and transient CL emission from this reaction it is ideally performed using a FIA manifold. Luminol CL can also be used as the basis for the determination of any metal ions that demonstrate catalytic properties in the reaction but, in order to achieve analytical selectivity, there is usually a need for on-line separation, as discussed in the next and subsequent sections on the determination of trace metal micronutrients.

3.3. Preconcentration techniques

Preconcentration can be used to improve sensitivity and to remove matrix interferences. For example, many solution phase CL methods for trace metal determination in seawater exhibit poor selectivity because Fe(II), Co(II), Cu(II) and Mn(II) are all known to catalyse luminol oxidation [60], and thus interfere by altering the relationship between luminescent emission and analyte concentration. Dissolved micronutrients are present in seawater in the pico- to nanomolar range, while the concentration of the major ions such as Na^{2+}, Ca^{2+} and Mg^{2+} are 10^6–10^{10} times greater. In addition, the seawater sample matrix, cations such as Ca^{2+}, Mg^{2+} may suppress trace metal CL emission relative to that for pure water standards, and may also precipitate as hydroxides under the alkaline conditions required for optimum CL. Solid phase preconcentration thus provides the *modus operandi* for both eliminating the interfering seawater matrix and enhancing the sensitivity, facilitating the detection of sub-nanomolar concentrations of micronutrients in seawater.

Chelating resins are a common medium for preconcentration of micronutrient trace metals in seawater [61]), and an often used solid phase is 8-hydroxyquinoline (8-HQ) immobilised on Toyopearl-TSK which shows high selectivity for transition and heavy metal cations relative to the major cations of seawater [62]. Toyopearl-TSK-8HQ microcolumns have been used in flow injection systems with CL detection for the determination of Fe(II) [63–65] Mn(II) [66], Co(II) [67] and Cu(II) [68] as discussed in the sections that follow. Similar FIA preconcentration procedures have

been used for sensitivity enhancement in seawater trace metal determinations using atomic spectrometric detection [69–72].

Analytical sensitivity may also be enhanced by preconcentration of an analyte after chromogenic reaction but prior to spectrophotometric detection. For example by extracting the phosphomolybdenum blue-cetyltrimethylammonium bromide (CTAB) ion pair onto a C_{18} resin, and then eluting with sulphuric acid, a detection limit of <2 nM was achieved in seawater using spectrophotometric detection [73].

4. Consideration of the schlieren (refractive index) effect in flow injection methods used in oceanographic analysis

The refractive index or schlieren effect occurs when light passes through a medium with refractive index gradients, resulting in the variable refraction of light into streaks [74]. In flow injection systems with spectrophotometric analysis, the schlieren effect can be quite problematic where the refractive index of the sample differs from that of the carrier stream into which it is injected. This arises because the interfacial boundary between the injected zone of one refractive index and the carrier solution of a differing RI will form parabolic liquid lenses at both the head and the tail of the injected sample zone. Light passing along the optical axis of a flow through detection cell will be refracted by these lenses to an extent dependent on the difference between the refractive indices of sample and carrier; this has the effect of dispersing or focusing light rays from the source either towards or away from the detector, causing artefact or schlieren peaks (Fig. 3a and b. This refractive index effect is well recognized in liquid chromatography, where tapered flow cells have been used to overcome it. However, in flow analysis it occurs even in the absence of a chromophore and, if ignored, can be a source of profound quantification errors [75].

In flow injection analysis of marine samples, the schlieren effect can be quite pronounced, especially where Z- or U-shaped photometric cells are used [40,76]. In the case of open oceanographic analysis, where there is no substantial difference in the salinity from one sample to the next, the simplest solution is to inject sample into a carrier of ultrapure seawater to ensure that there is no refractive index discontinuity between the carrier and injected sample. However, for estuarine samples, where the salinity can vary from 0 to 35 S, more involved solutions must be found. Some of these are listed in Table 1.

5. Method validation and data quality

Robust concepts and guidelines on data quality applicable to most types of measurements, including those on nutrients in seawater discussed herein, can be found in ISO/IEC 17025, the international standard establishing the “general requirements for the competence to carry out tests and/or calibrations, including sampling” [82]. It is implemented by laboratories worldwide seeking accreditation for their measurement activities. According to ISO/IEC 17025, “the validation shall be as extensive as is necessary to meet the needs of the given application or field of application”, and “may include procedures for sampling, handling and transportation”.

5.1. Method validation and uncertainty estimation

Method validation has been defined as “the confirmation by examination and the provision of objective evidence that the particular requirements for a specific intended use are fulfilled” [82]. A good understanding upfront of why the data is required and of what quality of the data is needed enables the setting of target uncertainties for the performance values under examination. A potentially robust approach to method validation is the use of appropriate certified reference materials (CRMs), but these are limited in number for macro- and micro-nutrients in seawater and have certified values significantly above those found in open ocean seawater. The ISO/IEC 17025 standard proposes four more approaches, alone or in combination: (i) the participation in interlaboratory comparisons, (ii) a comparison of results achieved with other methods, (iii) a systematic assessment of the factors influencing the results and (iv) an assessment of the uncertainty of the results based on scientific understanding of the theoretical principles of the method and practical experience.

Early intercomparison exercises for micronutrients in seawater [83,84] reported inconsistent results with up to an order of magnitude degree of variability in the quantification of the analytical blank and inaccuracies in system calibration. More recent intercomparison exercises have focused on Fe determinations [85,86] and reported that discrepancies observed between results, obtained using a variety of analytical methods, including FIA, remain too large. An ongoing comparison programme has since been undertaken for micronutrients using both FIA and other laboratory methods for the production of a seawater reference material [87]. The information provided on the sample collection and measurement procedures used is comprehensive but, beyond a reference value ± 1SD, no information on the statistical evaluation of the results, including acceptance/rejection criteria, is given. A recent intercomparison study for macronutrients in seawater also highlighted the difficulties associated with nitrite and silicate measurements [88], with the latter exhibiting larger consensus standard deviations than those obtained for nitrate and phosphate. The study also highlighted on-going problems with instrumental non-linearity. The long term stability of bulk open ocean seawater samples, collected as part of the Reference Materials for Nutrients in Seawater programme, has recently been assessed for nitrate, silicate and phosphate allowing these materials to be candidates for use as certified reference materials [89].

It is also potentially useful to compare results obtained from in situ or shipboard methods with results obtained from a laboratory reference method. Isotope dilution (ID) ICP-MS can be considered a possible reference method suitable for this purpose. As ID is based on the measurement of isotope ratios it is potentially more robust and less sensitive to problems specific for measurements at ultra-low levels, as exemplified by the measurement of Fe in seawater [86]. Ussher et al. compared the results for Fe determinations obtained by FIA-CL with ID-ICP-MS [87] and found good general agreement between the two methods over a concentration range of 0.15–2.1 nM Fe. There were however some discrepancies observed for some samples which were attributed to random effects, such as variable contamination, rather than systematic effects. However, ID-ICP-MS is not suitable for all analytes, e.g. nitrate and monoisotopic elements such as Co, Mn and P, which require alternative reference methods.

The factors that influence the uncertainty of the analytical result are multiple and may include sample collection, pre-treatment and storage as well as the other steps of the measurement process. A systematic identification and investigation of the entire measurement process requires competent, trained analytical chemists, a good understanding of the nature of the measurand and of the purpose of the measurements. Thus, a sound *a priori* understanding of the major sources of input to the measurement results, and of their associated uncertainty components, will help in identifying where efforts and resources need to be focussed to meet the target uncertainty. A best practice guide for performing macronutrient analysis at sea by SCFA has been produced [90] whilst a guide for micronutrient sampling and sample-handling is also available [91].

Uncertainty is defined as the ‘parameter, associated with the result of a measurement that characterises the dispersion of the

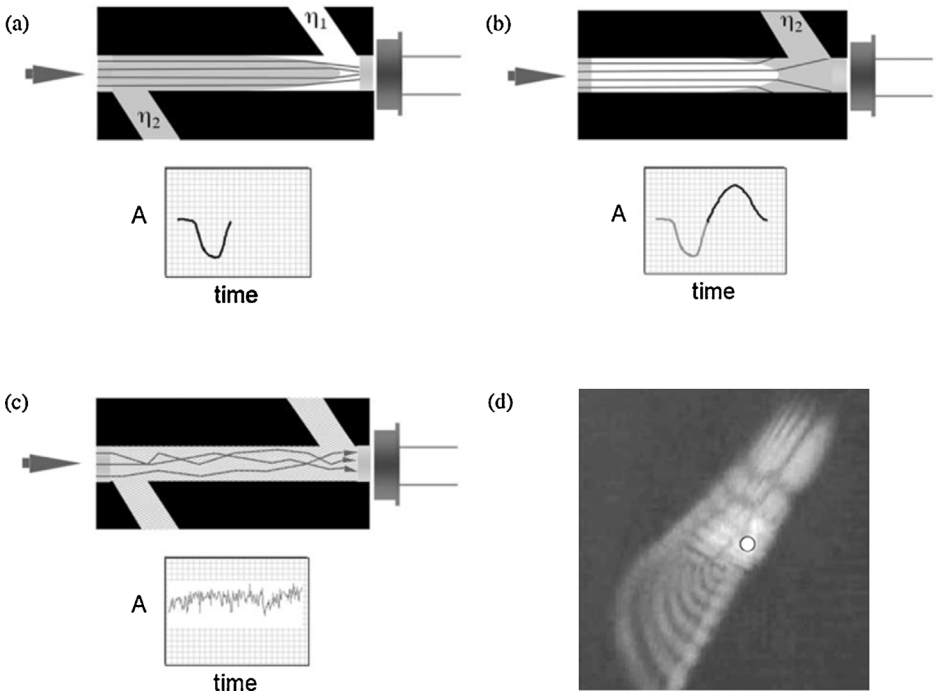

Fig. 3. Diagrammatic representation of refractive index effects in flow analysis. Parts (a) and (b) show the expected schlieren lensing effect when the RI of the sample zone, η_2, is higher than that of the carrier stream, η_1, whilst part (c) illustrates how liquid heterogeneity can cause additional detector noise. Part (d) is a projected image obtained by shining a 660 nm laser through a conventional flow-through cuvette (1.5 mm i.d., pathlength 10 mm), and injecting water with salinity of into a carrier of deionised water. The bright spot in the centre of the image corresponds to the aperture of the flowcell. Both the effects of schlieren lensing and liquid striation can be seen. The irregular shape of the image is apparently a function of non-uniform liquid flow within the flowcell. Figure and caption reproduced from Ref. [40] with permission.

values that could reasonably be attributed to the measurand' [92]. In practice, it is usually evaluated using a mathematical model of the measurement procedure and a numerical method of differentiation applied to combine the individual uncertainties associated with each parameter of the model, which should also include all corrections and correction factors. It should be noted that the uncertainty of a measurement is very different to the error; where error is the result of a measurement minus the 'true' value of the measurand [93] or, more generally and according to the international nomenclature, the "measured quantity value minus a reference quantity value" [92].

5.2. Measurement uncertainty in practice

The estimation of the uncertainty associated with an analytical measurement allows improved intercomparison of analytical results [94] and provides the strength of the links in the chain for traceability to national or international standards [92]. It is often the case that a simple statistical procedure is used to estimate the uncertainty of a measurement result. Typically, the internal instrumental precision obtained for analysis of a single sample, is calculated to give the range within which the stated result is likely to lie. This approach may however, underestimate the uncertainty of a measurement, leading to over interpretation of the significance of the result.

The Guide for Uncertainty in Measurements, often abbreviated to "the GUM", [95] has subsequently been interpreted for analytical chemistry by Eurachem [96] and sets out procedures for a holistic evaluation of uncertainty in analytical chemistry. This section uses the principles of these two guides to produce a worked example for simple measurement uncertainty estimations. The main stages in the process are identified as:

Table 1
A summary of different approaches used to overcome the schlieren effect in flow analysis.

Approach	Pros and cons	Reference
Individually **matching the carrier salinity** with that of each sample	Impractical where sample salinity is changing, e.g. estuarine waters.	
Performing **standard addition** on each sample	Impractical because of increased sample manipulation and reduced sample throughput.	
Using **large volume sample injections**, e.g. 1000 μL, and using only a central portion of the peak that is unaffected by the schlieren effects for quantification	Reduces sample throughput.	[77,78]
Using a **reagent injection** (reverse) flow method, where injected reagents are RI matched with a carrier that then merges with a continuous flow of sample, thus obviating any RI gradients.	Uses larger amounts of sample, but reagent consumption is small. Has been used in combination with LWCC for high sensitivity determination of phosphate [43].	[75]
Application of **dual or multiple wavelength spectrophotometry** to discriminate the schlieren signal from the combined analyte plus schlieren signal	For best results, scaling factors relating schlieren responses at the measurement and reference wavelengths must be determined [81].	[79]
Use of reflective or **multi reflection flow cells** in which the collimated light beam of the detector shines across the sample zone, either perpendicularly (single reflection), or at an angle (multi-reflection) minimizing the lensing effect of differing sample carrier refractive indices.	RI effect minimized, enhancement of optical path, stray gas bubbles not trapped.	[80] [31,32]

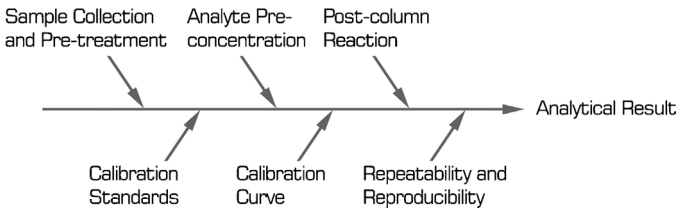

Fig. 4. Ishikawa diagram showing possible major uncertainty sources for the measurement of the dissolved Co concentration in seawater by FIA-CL.

- *specification – write down a clear statement of what is being measured, including the full expression used to calculate the result.*

In this case the measurand is the concentration of dissolved cobalt in seawater. The measurement method is based on the use of FIA-CL and the technique of standard additions. The proposed measurement equation is given by:

$$C_{DCo} = \frac{I_S - I_B}{b} \quad (2)$$

where C_{DCo} is the concentration of dissolved Co in pmol/kg, I_S is the intensity of the sample signal in V, I_B is the intensity of the blank signal in V and b is the slope of the calibration curve in V pmol^{-1} kg. Note that parameter b will have been calculated using regression analysis of data obtained from the seven calibration standards analysed.

- *identify uncertainty sources – produce a list of all the sources of uncertainty associated with the method.*

This is often initially achieved visually using an Ishikawa or cause and effect diagram [97] showing the major expected sources of uncertainty. The diagram typically contains a branched hierarchical structure reducing to a single outcome, in this case an analytical result. Elements within the structure may contain uncertainties from sources such as analyte recovery (including extractability), measuring devices (e.g. tolerances for balances, pipettes and volumetric ware, dilution errors), calibration, temperature and internal standards errors, which are then combined using uncertainty propagation laws. For this example six possible major uncertainty sources have been proposed and are shown in Fig. 4.

In an ideal world replicate samples would be taken at each sampling point to allow the effects of sample collection and pre-treatment to be considered. In practice however this is not undertaken for open ocean and coastal work due to constraints on water budgets and the sampling systems used. Thus, whilst sample collection is likely to contribute to the overall uncertainty it will not be considered further here.

- *quantify uncertainty components – measure or estimate the magnitude of the uncertainty associated with each potential source of uncertainty identified.*

Three components are required in Eq. (2) for the calculation of the concentration of cobalt in a sample, the signal intensity of a seawater sample, sample RC1, and the blank and the slope of the calibration curve. The former two were estimated from averaged measurement results ($n = 3$) and were found to be 2.280 ± 0.070 and 0.0863 ± 0.0095 V respectively whilst the slope was 29.41 ± 0.70 V pmol^{-1} kg. The uncertainty on the slope results from the combination of the uncertainty of the concentration of cobalt in each of the calibration standards and the uncertainty on the measured intensities for the calibration standards analysed. In theory the former should be small [98], provided that high quality volumetric ware or gravimetrically prepared standards are used. Worked examples to calculate the uncertainty of a calibration standard are given elsewhere [94,96].

From separate experiments the intermediate precision of the method, P, was assessed by analysing two different open ocean seawater samples, one from the surface and one from depth, with cobalt concentrations of 35 and 65 pmol kg^{-1}, 12 times each over a period of 3 months. This data gave an intermediate precision for the method of 14% relative (1 SD).

- *calculate the combined uncertainty – combine the individual uncertainty components, following the appropriate rules, to give the combined standard uncertainty for the method; apply the appropriate coverage factor to give the expanded uncertainty.*

Using the sample and blank intensity values and the slope of the calibration curve the concentration of dissolved cobalt in a separate sample (labelled RC1) was calculated to be 75 ± 5.9 pmol kg^{-1}, using a coverage factor, k, of 2 (which given sufficient degrees of freedom, approximates to the 95% confidence interval [95]), for the uncertainty estimation. This estimation was made using the spreadsheet method of Kragten [99] with Eq. (2) used as the calculation model. To illustrate the effect of each parameter in the model on this estimated combined uncertainty, their individual uncertainty estimates were included sequentially in the calculations, giving three separate results. The results of these calculations are shown in Table 2 along with the effect that each individual uncertainty has on the combined uncertainty. For the first two scenarios given, the uncertainty is dominated by the precision of the sample signal intensity, I_S, contributing 100 and 98% respectively, with a minimal contribution from the blank intensity in scenario 2. In scenario three the relative contribution from I_S decreases to 65% as the uncertainty of the calibration curve slope is introduced into the calculations. This results in an increase in the estimated combined uncertainty ($k = 2$) from 4.8 to 5.9 pmol kg^{-1}, i.e. from 6.5 to 8% relative.

The basic purpose of an uncertainty statement is to propose a range around the measurement result that encompasses the 'true' value or the range of possible 'true' values. To stand a chance of being meaningful, any estimated combined uncertainty must be at least as large as the known variability of the measurement result. It is not necessarily easy to be able to guarantee the correctness of an uncertainty estimation as this depends on the way the factors influencing this measurement result and its associated uncertainty are understood and/or perceived. However, it is quite simple to verify compliance with the minimum acceptance criterion described above.

In the current example, the comparison between the relative combined standard uncertainty ($k = 1$) estimated for the Co concentration (4%) with the relative intermediate precision described above (14%) shows that this basic condition is not met. This is an indication that one or more sources of uncertainty have not yet been properly identified and propagated through to the final uncertainty estimate. The consistency of the analyte pre-concentration step and the stability of the post column chemiluminescence reaction appear as possible candidate additional important sources of measurement uncertainty. The short term stability of these two parameters would have been accounted for by the internal precision obtained for analysis of a single samples and by monitoring instrumental drift during an analytical run. However, the longer term effects would not be accounted for by this approach. The realistic assessment of these two uncertainty sources would require a systematic investigation of the FIA-CL system, e.g. by using off-line sample buffering, off line pre-concentration and replacing the pre-concentration column with a sample loop, which would be time consuming and hence costly. An alternative would

Table 2
Uncertainty estimates and contributions for the determination of dissolved Co (DCo) in seawater, where U is the estimated expanded combined uncertainty ($k = 2$) and REU is the relative estimated expanded combined uncertainty.

Scenario	Parameters included in uncertainty model	[Co]/pmol kg^{-1}	U([Co])/pmol kg^{-1}	REU([Co])/%	Individual contribution to the estimated uncertainty/%		
					Sample Intensity (I_S)	Blank Intensity (I_B)	Calibration curve slope (b)
1	I_S	75	4.8	6.4	100		
2	I_S and I_B	75	4.8	6.5	98	2	
3	I_S, I_B and b	75	5.9	8.0	65	1	34

thus be to use the intermediate precision estimate as the minimum uncertainty estimate.

In summary, a systematic investigation of the measurement process, but excluding sample collection and pre-treatment effects, has shown that the uncertainty of a measurement is often underestimated, increasing here from 6.4% relative for a simple precision measurement of an individual sample to 8% when further parameters of the measurement equation are included to 28% when longer term precision data (2 SD) is used as the uncertainty estimate, and has also highlighted which areas of the analytical method need further refinement. This leads the analyst to ask the following questions "What can I do to reduce the uncertainty associated with the calculation of the slope?" and "What can I do to reduce the influence of the factors likely to reveal themselves on a long term basis?" Thus, the benefit arising from the estimation of an uncertainty budget is that it enables a more realistic identification of the major uncertainty contributors, and focus efforts to minimise them [100].

6. Macronutrients

6.1. Phosphorus

Phosphorus occurs in water in dissolved forms (defined as the 0.2 or 0.45 μm filterable fraction), mostly as inorganic orthophosphates and condensed or polyphosphates, but also as organic phosphates (phosphoproteins and nucleic acids, phospholipids, phosphoamides, sugar phosphates, inositol phosphates, aminophosphonates and P-containing pesticides, as well as colloid associated inorganic and organic P). Particulate P is comprised of clay and silt-associated organic and inorganic P, precipitates of authigenic origin and P-containing biological matter [101].

6.1.1. Dissolved reactive phosphorus

Dissolved inorganic P is most commonly determined as *dissolved* reactive P (DRP), i.e. the fraction that reacts with acidic molybdate to form molybdophosphate which is then reduced to the strongly absorbing phosphomolybdenum blue complex [102]. Total or total dissolved P must be first digested with both acid and a strong oxidant to convert all P forms to detectable orthophosphate [103].

One of the earliest applications of FIA to the determination of DRP in marine systems was reported by Johnson and Petty [104]). In this system, reagent injection ("reverse FIA") was used to inject a combined colorimetric reagent, resulting in reagent savings, arguably higher sensitivity and a greater suitability for on-line monitoring applications. Subsequently a similar approach for DRP determination was adopted by Lyddy-Meaney et al. [37] who developed a portable, multicommutated spectrophotometric FIA system that included on-line tangential-flow filtration (0.2 μm) and was suitable for rapid underway deployment. At a sample injection rate 225 h^{-1} and a vessel speed of 30 knots, a spatial resolution of ca. 250 m over a cruise track of ca. 150 km was achieved.

Sequential injection analysis, because of the manner in which sample and reagents are sequenced, and the need for flow reversal, has often been considered to have lower sample throughput than FIA. However, Frank et al. [105] have demonstrated a SIA system for DRP determination that used detection of fluorescence inhibition of the rhodamine 6G-molybdate ion association complex by phosphate to achieve a high sample throughput of 270 h^{-1} with a LOD of 0.05 μM (Fig. 5). This system was used effectively for surface water transect measurements in the North Sea, Wadden Sea and Elbe estuary.

Flow analysis methods that are suitable for freshwater analysis do not necessarily translate successfully for use in marine and estuarine samples because of the high ionic strength and presence of potentially interfering cations and anions in the sample matrix. For example, Udnan et al. [106] reported a flow injection system for the determination of DRP that used amperometric detection of phosphomolybdate after a 2 min in-valve preconcentration on a small anion exchange column (Table 3). A LOD of 0.18 μg L^{-1} P (6 nM) was achieved using this approach, but the method was only suitable for pristine freshwaters because the preconcentration efficiency diminished markedly at chloride concentrations >1.4 mM. Liang et al. [73] have reported a flow injection preconcentration technique that is more suited to detection of DRP in marine waters. This involved solid phase extraction of the phosphomolybdenum

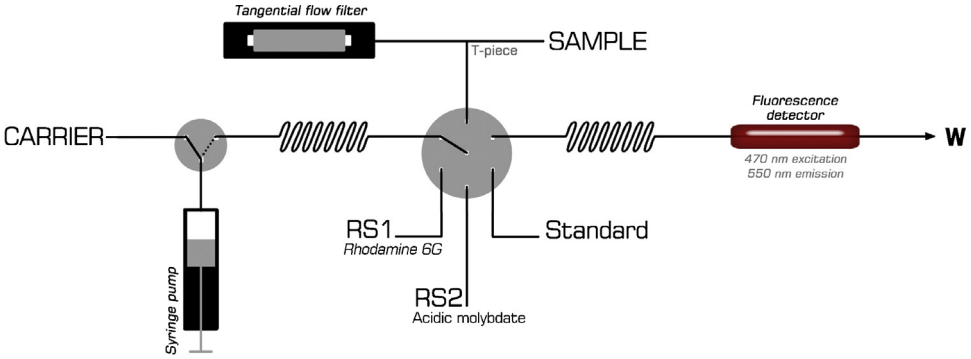

Fig. 5. Schematic of the SIA used for phosphate analysis. Samples for comparative laboratory analysis were taken from the stream leaving the cross-flow filter. Redrawn from Ref. [105], with permission.

Table 3
Summary of flow analysis techniques used for macronutrients determinations in marine and estuarine waters.

Parameter	Flow mode	Basis of method	Analytical performance	Notes	Ref.
Phosphorus					
DRP	FIA	Reagent injection with spectrophotometric detection of phosphomolybdenum blue.	LOD 0.05 μM Repeatability: 4.5% RSD (0.75 μM) 1.5% RSD (3 μM) Throughput: 90 inj h^{-1}		[104]
DRP	FIA	Multicommutation with spectrophotometric detection of phosphomolybdenum blue.	LOD: 0.15 mM Repeatability: 1.95% RSD (n = 9) Throughput: 225 inj h^{-1}		[37]
DRP	SIA	Fluorescence inhibition of phosphate on rhodamine 6G-molybdate ion pair formation.	LOD 0.05 μM Throughput: 270 inj h^{-1}		[105]
DRP	FIA	Preconcentration of orthophosphate on amperometric detection of phosphomolybdate.	LOD: 3.4 μg P L^{-}1 (0.11 μM) 70 inj h^{-1}	Not applicable to waters with chloride > 1.4 mM	[106]
DRP	FIA	Removal of sulphide interference in phosphomolybdate spectrophotometric method by the use of a $KMnO_4$ carrier.	LOD: 37 μg P L^{-1} Repeatability: 2.5% RSD (n = 3)	No interference caused by oxidation by permanganate of a range of organic P compounds found in natural waters.	[109]
DRP	FIA	Spectrophotometric detection of phosphomolybdenum blue using 1 m liquid waveguide capillary cell (LWCC).	LOD: 10 nM Linear range: 0.1–1 μM Repeatability: 7% RSD (n = 3) Throughput: 18 inj h^{-1}	A sample injection of twice the LWCC volume was used to avoid schlieren effects.	[41]
DRP	FIA	Reverse FIA spectrophotometric detection of phosphomolybdenum blue using 2 m liquid waveguide capillary cell (LWCC).	LOD: 0.5 nM Linear range: 0–160 nM Repeatability: 1.54% (24.7 nM, n = 9) 1.86% RSD (82.5 nM, n = 9) Throughput: 15 inj h^{-1}	Reverse FIA configuration used to avoid schlieren effect.	[43]
DRP	FIA	Solid phase extraction of phosphomolybdate-CTAB ion pair on C18, followed by elution and chemiluminescence detection with luminol.	LOD: 0.002 μM Linear range: 0.005–0.194 μM Repeatability: 4.77% RSD (0.097 μM, n = 7) Throughput: -	Negligible interference from Si, good agreement with MAGIC method. Luminescence response affected by salinity.	[250]
DRP	FIA	Solid phase extraction of phosphomolybdenum blue-CTAB ion pair on C18, followed by elution and spectrophotometric detection.	LOD: 1.57 nM Linear range: 3.2–48.5 nM Repeatability: 4.52% RSD (32.4 nM, n = 8) Throughput: 2 h^{-1}	Negligible interference from Si, good agreement with MAGIC method.	[73]
DOP	FIA	UV photo-oxidation using peroxodisulphate with photometric detection of phosphomolybdenum blue.	LOD: 10 μg P L^{-1} (0.32 μM) Repeatability: ≤ 1.9% RSD for DRP ≤ 5.0% RSD for DOP Throughput: 22 inj h^{-1}		[116]
DOP	SCFA	UV photo-oxidation using hydrogen peroxide with photometric detection of phosphomolybdenum blue.	LOD: 0.02 μM Linear range: Repeatability: 0.007 μM (σ_{n-1}, n = 3) for ≤6 μM range.		[121]
TP	FIA	UV + thermal photo-oxidation using peroxodisulphate with photometric detection of phosphomolybdenum blue	LOD: 1 μg P L^{-1} (0.032 μM) Repeatability: 4.6% RSD (100 μg P L^{-1}, n = 10). Throughput: 115 inj h^{-1}	Suitable for a wide range of salinities; 2499 measurements made in 25 hr period.	[34]
Nitrogen					
Nitrate	FIA	Nitrate reduced to nitrite using Cu(Cd) reductor; nitrite determined with Griess reagent.	LOD: 0.1 μM Repeatability: 1% RSD (≥10 μM) Throughput: 75 inj h^{-1}		
Nitrate	FIA	Nitrate reduced to nitrate using Zn reductor at pH6.5; nitrite determined with Griess reagent.	LOD: 1.3 μg N L^{-1} (0.093 μM) Linear range: 3–700 μgL^{-1} NO_3–N Repeatability: 1.2% RSD (50 μgL^{-1} NO_3–N, n = 10). Throughput: 40 inj h^{-1}	>3200 measurements made over 285 km cruise path.	[33]
Ammonia	FIA	Gas diffusion with spectrophotometric detection	LOD: 0.05 μM Linear range: 0.1–10 μM Repeatability: ≤2% RSD (2 μM, n = 28). Throughput: 60 inj h^{-1}		[144]

Table 3 (*Continued*)

Parameter	Flow mode	Basis of method	Analytical performance	Notes	Ref.
Ammonia	FIA	Hybrid reagent-injection FIA system utilising gas diffusion with spectrophotometric detection	Continuous flow mode: LOD: 9 μg N L^{-1} (0.6 μM) Linear range: 20–160 μg N L^{-1} Repeatability: 3% RSD (at 100 μg N L^{-1}, $n = 3$) Throughput: 135 inj h^{-1} Stop-flow mode: LOD: 3 μg N L^{-1} Linear range: 20–160 μg N L^{-1} Repeatability: 2% RSD (100 μg N L^{-1}, $n = 3$) Throughput: 60 inj h^{-1}		[145]
Ammonia	FIA	Gas diffusion with fluorescence detection using OPA reagent	LOD: 7 nM Linear range: Repeatability: 5.7% (800 nmol L^{-1}, $n = 24$). Throughput: 30 inj h^{-1}.		[50]
Total dissolved nitrogen	FIA	UV photo-oxidation using peroxodisulphate with photometric detection of nitrate using Cd reduction and Griess reagent	LOD: 0.03 mg N L^{-1} (2.14 μM) Linear range: <3 mg N L^{-1} Repeatability: 0.47% RSD (1 μg N L^{-1}, $n = 8$) Throughput: 8 samples h^{-1} (triplicate injections)	Sample digested in continuous UV reactor, then injected into detection manifold to minimize degradation of Cd-reductor.	[151]
Carbon					
DIC	FIA	Gas diffusion with conductimetric detection.	LOD: <0.1 mM Linear range: <0.1–20 mM Repeatability: 1.4% RSD (2 mM)	Zn^{2+} added to eliminate interference from H_2S in anoxic samples.	[142]
DIC	FIA	Gas diffusion with C^4D and spectrophotometric detection, respectively.	LOD: 0.12 mM Linear range: 0.5–5 mM Repeatability: 0.46% RSD (6 mM, $n = 9$) Throughput: 90 inj h^{-1}	>250 measurements during a 4 hr cruise.	[166]
DIC and p_{CO_2}	FIA	Gas diffusion with conductimetric detection	LOD: 2.9 μmol kg^{-1} Linear range: Precision: 10% Accuracy: −3.3% Throughput: inj h^{-1}		
Dissolved organic carbon, dissolved inorganic carbon	SIA	UV photo-oxidation of organic C; gas diffusion and spectrophotometric detection of CO_2 produced	LOD: 0.05 mg C L^{-1}. Linear range: 0.05–5.0 mg C L^{-1} for both DIC and DIC + DOC. Repeatability: 5.3% RSD [DIC], ≤ 6.6% [DIC + DOC] (0.05 mg C L^{-1} $n = 3$). Throughput: 8 inj h^{-1}	Interference from Cl^- at >100 mg L^{-1} (due to formation of Cl_2?)	[178]
DIC and p_{CO_2}	FIA	Gas diffusion with C^4D and spectrophotometric detection, respectively.	LOD: 0.12 mM (DIC), 114 μatm (p_{CO_2}). Linear range: 0.5–5 mM (DIC), 154–3832 μatm (p_{CO_2}) Repeatability: 0.46% RSD (6 mM, $n = 9$) (DIC), 0.8% RSD (at 365 μatm, $n = 3$) Throughput: 90 inj h^{-1}	>250 measurements of each made in 4 hr cruise.	[166]
Total alkalinity	SIA	SIA titration with photometric detection and peak width measurement	LOD: 5.1 HCO_3^- L^{-1} Linear range: 10–50 mg HCO_3^- L^{-1} Polynomial calibration range: 10–50 mg HCO_3^- L^{-1} Repeatability: 0.4% RSD (27 mg HCO_3^- L^{-1}) 0.3% RSD (76 mg HCO_3^- L^{-1}) Throughput: 65 inj h^{-1}		[172]
Total alkalinity	FIA	Gas diffusion of CO_2 produced by addition of pH 4.5 buffer.	LOD: 40 μM Linear range: 800–3200 μM Repeatability: 1% RSD (at 3200 μM, $n = 9$) Throughput: 71 inj h^{-1}	Used for surface (0.2 m) subsurface (1 m) underway measurements.	[173]
Silicon					
Silicate	FIA	Reverse FIA system with spectrophotometric detection of silicomolybdenum blue. Ascorbic acid and tin(II) chloride used as reductants.	LOD: 0.5 μM Repeatability: 1% RSD (at ≥10 μM) Throughput: 80 inj h^{-1}	Underway measurement at 60 hr^{-1} of water from 2 m depth. Slight salinity error when tin(II) chloride used as reductant.	[181]

Table 3 (*Continued*)

Parameter	Flow mode	Basis of method	Analytical performance	Notes	Ref.
Silicate	FIA	FIA system with spectrophotometric detection of silicomolybdenum blue. Tin(II) chloride used as reductant, with dual wavelength photometric detection.	LOD: 0.3 μM Repeatability: 1% RSD (at ≥5 μM) Throughput: 60 inj h^{-1}	No significant salinity error between 28 and 34 S (PSS78). Designed for use in submersible system.	[180]
Silicate	SIA	Spectrophotometric detection of silicomolybdate using a 2 m liquid core waveguide.	LOD: 0.1 μM Linear range: 0.1–10 μM. Throughput: 4 inj h^{-1}	Salinity correction algorithm applied to data.	[182]
Silicate	FIA	Spectrophotometric detection of silicomolybdenum blue using a 1.6 m LCW liquid core waveguide. Ascorbic acid used as reductant.	LOD: 9 nM Repeatability: 1.5% RSD (at 250 nM, $n = 7$) Throughput: 12 inj h^{-1}	No significant salinity effect on signal.	[44]

blue – cetyl trimethylammonium bromide ion pair on a C_{18} column. After elution with ethanol and sulphuric acid, detection was achieved using spectrophotometry. A limit of detection of 1.57 nM was achieved but the sample throughput was only 2 h^{-1}.

FIA can also be used advantageously to remove interferences. The determination of DRP in the anoxic pore waters of estuarine sediments should be performed without exposing samples to the atmosphere in order to avoid changes in the redox condition, and FIA is ideally suited to this task. However, even when performed under anoxic conditions, the determination is fraught with interferences that are ascribed to the presence of sulphide, which either interferes in the phosphomolybdate reduction step [107] or competes with phosphate in complexing with molybdate [108]. Grace et al. have described a modification to the DRP method that involved on-line pre-oxidation of sulphide with permanganate prior to spectrophotometric detection [109]. This approach proved to be successful, and the selectivity of the analysis was not compromised by oxidation of organic P species commonly found in pore waters.

6.1.2. Total phosphorus and dissolved organic phosphorus

There is increasing interest in the dynamics [110–112] and bioavailability of dissolved organic phosphorus in estuaries and the oceans [113], and this has emphasised the need for the development of convenient, reliable and rapid methods for the determination of dissolved organic phosphorus (DOP) and the associated parameters, total dissolved phosphorus (TDP) and total phosphorus (TP), as well as methods for the quantification of different P-species.

The determination of dissolved organic phosphorus and total phosphorus requires that these components first be converted to orthophosphate by a combination of dissolution, hydrolytic and oxidative processes before detection as phosphomolybdenum blue [114]. When performed by classical batch digestion this process is slow, but the process can be performed rapidly by flow analysis techniques, and a number of FIA systems using UV photo-oxidation with peroxodisulphate [115,116] alone or in conjunction with acid hydrolysis [117,118], or microwave digestion [119,120] have been described for use in fresh and wastewaters. For samples such as soil waters, Peat et al. [118] found that acidic photo-oxidation was required to avoid interference from higher concentrations of Fe and Al which can complex with phosphate. For marine waters, Aminot and Kerouel [121] reported that 5–6-fold dilution of sample was required in a SCFA photo-oxidation method for dissolved organic phosphorus in order to achieve full recovery of a series of model organic P compounds. This matrix effect was presumably due to interference from the high concentrations of Ca and Mg ions in seawater.

Gentle et al. addressed the problem of photo-oxidation inhibition by the seawater matrix, and found that complete digestion of total phosphorus could be achieved over the whole salinity range in a FIA system if a combined photo-oxidation – thermal digestion procedure was adopted [34]. This FIA system (Fig. 6, Table 3) was capable of 115 measurements per hour, with a LOD of 1 μg L^{-1} P (0.03 μM), and used to perform 2499 underway TP measurements during a cruise in the coastal waters of Victoria, SE Australia.

6.2. Nitrogen

Nitrogen occurs in aquatic systems in dissolved inorganic forms (DIN = Σ[nitrate + nitrite + ammonia]) and as dissolved organic nitrogen (DON) which includes species such as urea, amino acids, amines, amino sugars, purines, pyrimidines, nucleosides nucleotides, proteins and polypeptides. Particulate N which is almost entirely organic N, i.e. TPN ≈ PON [122], is determined by the difference between total nitrogen (TN) and total dissolved nitrogen (TDN). Along with micronutrients like iron, nitrogen is a limiting macronutrient in the oceans [123].

6.2.1. Nitrate

Traditional methods for the determination of nitrate in marine waters are based on the heterogeneous reduction of nitrate to nitrite using copperised Cd and subsequent colorimetric determination of the nitrite formed [124] by the Griess reaction, i.e. diazotization with sulfanilamide followed by coupling with N-(1-naphthyl)-ethylenediamine dihydrochloride (NED) to form a pink azo dye [125]. Johnson and Petty [126] first described the use of FIA for nitrate measurement in marine waters using Cd reduction and the Griess reaction for nitrite detection, and their work has been adapted by many for surface [127] and submersible systems [27,128–131].

Despite the fact that the most widely used segmented continuous flow [132] and flow injection analysis [27,126,127] methods for nitrate determination utilize copperised cadmium granule columns or Cd tubes, use of cadmium reduction is often unreliable due to over-reduction to hydroxylamine and ammonia, or because column poisoning causes diminished reduction efficiency [133,134]. Cadmium use is also undesirable because of potential occupational health issues and the production of toxic waste, and hence use of an environmentally benign reductant is preferred. Alternative reduction strategies have included the use of hydrazine [135,136] and photo-reduction [137,138], but neither can be used successfully in seawater.

Ellis et al. [33] have described a field portable, reagent injection, flow analysis system that utilized a Zn reduction column at pH 6.5 in conjunction with the Griess reagent for the spectrophotometric detection of nitrate (Fig. 7a). The advantage of using Zn at this pH

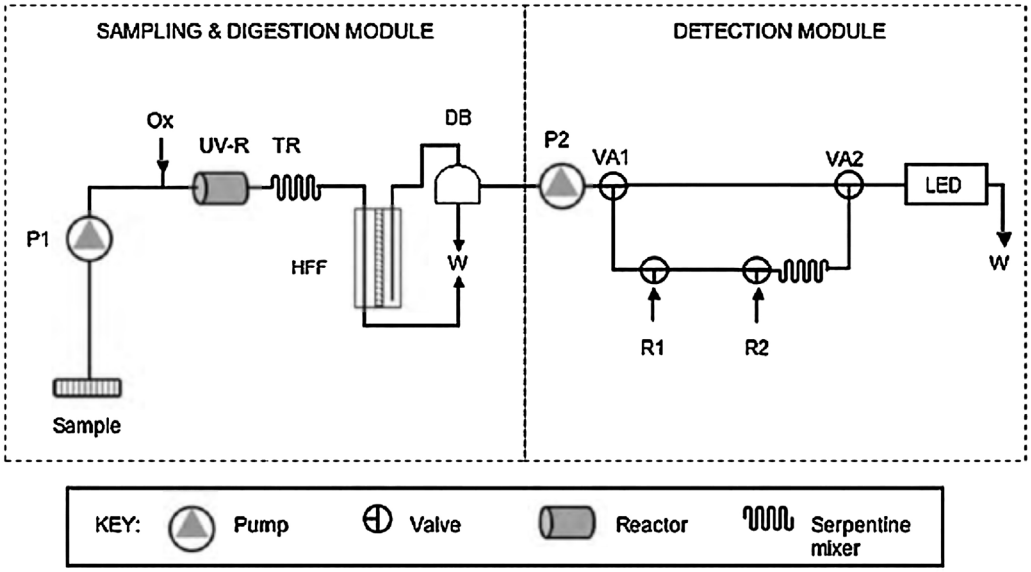

Fig. 6. Diagrammatic description of the flow analysis system used for the determination of total phosphorus. Sample is pumped through a 100 μm mesh, followed by the addition of acidic peroxodisulphate oxidant (Ox). P1 and P2 are peristaltic pumps. The stream undergoes mineralisation in the UV reactor (UV-R) and a thermal reactor coil (TR) followed by filtration using a hollow fibre filter (HFF) and debubbling (DB). Overflow from the debubbler goes to waste (W). Filtered digested sample is pumped into a reagent injection flow analyser where reagents (R1 – acidic molybdate and R2 – acidic tin(II) chloride reductant) are delivered into the stream. Absorbance is measured using a multi-reflective cell coupled with a 660 nm light emitting diode source. Reproduced with permission from Ref. [34].

is that there is no problem with precipitation of Ca or Mg ions in seawater, which can occur when reduction is performed at higher pH (e.g. with Cd). The method was suitable for waters with a wide range of salinities and was successfully used to obtain more than 3200 nitrate measurements during deployment in Port Phillip and Westernport Bays, in SE Australia (Fig. 7b).

However, as is the case with the copperised cadmium reduction procedure, the mechanism of the Zn reduction of nitrate to nitrite is still not clearly understood. Zn columns require activation with a higher concentration (e.g. 500 $\mu g\,L^{-1}$ NO_3–N) for ca. 30 min until a stable response is achieved [139] (cf. Fig. 8a). Thereafter, columns perform quantitative reduction of nitrate to nitrite for many hundreds of injections (Fig. 8b). If a column is conditioned with nitrite rather than nitrate (Fig. 8a), the same trend is observed. Since the photometric detection system is specific for nitrite, this implies that initially both nitrite and nitrate are reduced, probably to ammonia, until some quasi-equilibrium state is reached where quantitative nitrate to nitrite reduction is achieved.

Whilst the Zn reduction method has some arguable advantages vis-à-vis the commonly used copperised cadmium method, both methods rely on a metastable reduction step prior to spectrophotometric detection using the Griess reaction. There is a real need for the development of a suitable chromogenic reagent or method that is selective for nitrate per se across a wide range of salinities.

6.2.2. Ammonium

At the pH of seawater, ammonia occurs predominantly in the ammonium form. Several approaches have been used in the automated detection of this species in marine waters. The most common SCFA method involves the reaction of ammonia with hypochlorite and subsequently with phenol to form indophenol blue that is then determined by photometry [124]. Interferences include volatile amines and a chelating agent is required to complex magnesium and calcium ions to avoid their precipitation under reaction conditions. A different, more sensitive approach utilizes the fluorescence of the reaction between ammonia and orthophthaldialdehyde (OPA) in the presence of sulphite, and this has been extensively used in SCFA [140].

Another approach favoured in FIA involves the use of a gas diffusion technique, in which ammonium is converted to volatile ammonia that diffuses across a gas permeable membrane into an acceptor solution. The diffused ammonia is typically detected by measuring the resultant change in conductivity of a deionised water [141] or dilute acid acceptor stream [142], or of the absorbance of a lightly buffered acceptor containing a pH indicator [143]. However, in order to the gas diffusion approach to work, ammonium must be converted to volatile ammonia by merging the sample with base, but in seawater this is problematic because calcium and magnesium ions precipitate under alkaline conditions, causing blockages in the flow system. Willason and Johnson [144], who were among the first to demonstrate the use of FIA for ammonia determinations in seawater, addressed this problem by the addition of citrate to complex these ions prior to gas diffusion. Gray et al. [145], however, minimized the extent of Mg and Ca hydroxide precipitation prior to gas diffusion by the use of a hybrid reagent injection system in which microlitre volumes of base were injected into a continuous flow of sample.

Watson et al. [50] combined gas diffusion separation with the OPA-ammonia reaction and used fluorescence detection to achieve very low detection limits (7 nM) for ammonia determination in seawater (see Table 3). Volatile, low molecular-weight amines were found to diffuse less efficiently through the membrane and did not react appreciably with OPA when sulphite was used as the reductant, and hence did not interfere in the method.

6.2.3. Total nitrogen and total dissolved nitrogen

In order to determine total nitrogen (TN) or total dissolved nitrogen (TDN), all nitrogenous substances must be completely converted to a single detectable species such as nitrate or ammonium. Historically the Kjeldahl method involving catalysed digestion with concentrated sulphuric acid was most commonly used to mineralise organic nitrogenous species to ammonium [146], which was then quantified by titration or colorimetry, and more recently by SCFA [147] and FIA [141]. However, this method only measures organic nitrogen and ammonium, requiring that NOx be measured separately in order to measure TN/TDN, and

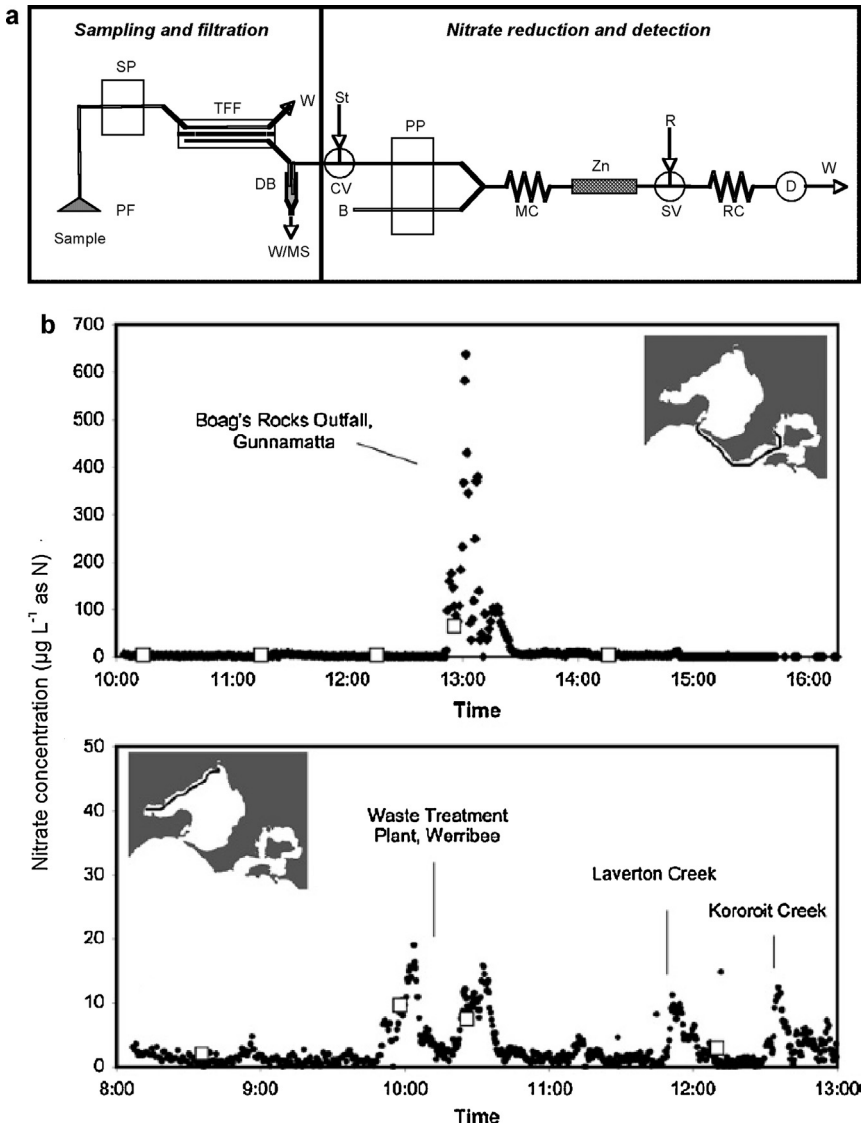

Fig. 7. (a) Reverse flow injection manifold used for the determination of nitrate. Key: PF, prefilter; SP, sampling pump; TFF, tangential flow filter; W, waste line; DB, debubbler; W/MS, waste/manual sampling line; St, standard; CV, calibration valve; PP, peristaltic pump; MC, mixing coil; ZnC, zinc column; R, Griess reagent; SV, solenoid valve; RC, reaction coil; D, detector. (b) Spatial concentration plots showing the location of point source inputs into Port Philip Bay and Bass Strait. Reproduced with permission from Ref. [33].

for this reason alternative approaches that oxidized all N present gained favour for seawater analysis. Both thermal digestion [148] or UV photo-oxidation [149] coupled with an oxidant such as peroxydisulphate have been used extensively, where the final product, nitrate is determined spectrophotometrically using Cd-reduction and the Griess reaction. Whilst automation of the UV or thermal digestion and detection steps for TN/TDN determination using both SCFA and FIA/SIA have been described for waters and wastewaters, the approach is not without its limitations. In batch digestion methods the digestion period is sufficiently long (hours) that peroxydisulphate oxidant is completely converted to sulphuric acid [150], whereas in automated methods the UV or thermal exposure time required for complete oxidation of N-species is short (10s of seconds) and there remains a high residual concentration of peroxydisulphate which can potentially damage the reduction column. For example, McKelvie et al. [151] used UV photo-oxidation with alkaline peroxydisulphate to completely convert dissolved N species to nitrate which was detected by spectrophotometry after Cd-reduction and diazotization. To avoid degradation of the Cd column by continuous contact with the high concentration of $S_2O_8 2-$ required to achieve complete digestion, photo-oxidation was performed in a separate sub-manifold, and only a small volume of digested sample was injected into the detection sub-manifold. Cerda et al. [152] used hydrazine as an alternative reductant to Cd following microwave digestion with peroxydisulphate, but their method was not applied to marine samples.

Nitrate produced by UV-photo-oxidation or thermal digestion of organic-N species can also be detected by UV spectrophotometry at ca. 220 nm but the spectral overlap between residual peroxodisulphate and nitrate in the 200–230 nm region is problematic, limiting the sensitivity of the method. Techniques such as second derivative spectrometry [35], spectral multi-component analysis [153], and single wavelength measurement with residual peroxodisulphate blank correction [154] have been used in conjunction with FIA techniques to overcome the problem of the large peroxodisulphate background signal. Whilst these approaches have been demonstrated for the determination of TDN in fresh and

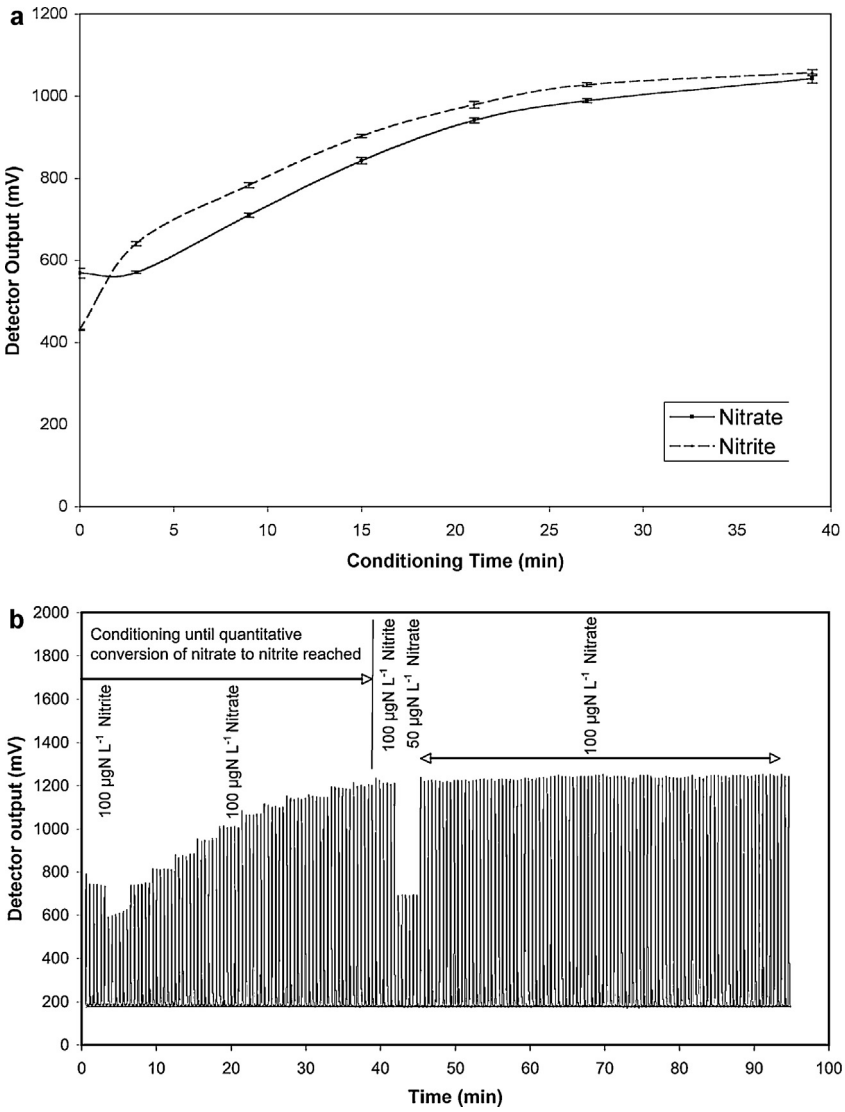

Fig. 8. (a) Plot showing detector response when nitrite and nitrate (both 500 $\mu g\,L^{-1}$ N) were used to condition a Zn reductor column. (b) Detector response plot showing when a Zn column was conditioned with 100 $\mu g\,L^{-1}$ N nitrate for ca. 40 min followed by a period of constant analytical response for 100 $\mu g\,L^{-1}$ N nitrate and nitrite standards. [139].

wastewaters, none have been successfully applied to seawater because of additional spectral interference from the saline sample matrix.

6.3. Carbon

The total carbon (TC) content of water can be can be divided into total organic carbon (TOC) and total inorganic carbon (TIC), and further classification into dissolved (filterable) and particulate forms is often performed. In seawater the concentration of inorganic carbon is usually several orders of magnitude greater than organic carbon [155].

Measurement of dissolved carbon dioxide species and pH in marine systems is of topical interest because of their major role as a sink for anthropogenic carbon dioxide [156] and because of concerns about ocean acidification in response to the increased partial pressure of CO_2 in the atmosphere [157].

Dissolved inorganic carbon (DIC), also referred to as total carbonate, T_{CO_2} or $\sum CO_2$, consists of dissolved carbon dioxide ($CO_{2(aq)}$), bicarbonate (HCO_3-) and carbonate (CO_32-) plus carbonic acid (H_2CO_3) which is usually <0.3% of $[CO_{2(aq)}]$. These species occur in pH-dependent equilibria as shown [158]:

$$CO_{2(g)} \rightleftharpoons CO_{2(aq)},\ pK_H = 1.47 \text{at} 298\,K, S = 0, \text{from which} pCO_2 = K_H[CO_{2(aq)}].$$

$$CO_{2(aq)} + H_2O \rightleftharpoons HCO_3- + H^+,\ pK_{a1} = 6.35 \text{at} 298\,K, S = 0$$

$$HCO_3- \rightleftharpoons CO_32- + H^+,\ pK_{a2} = 10.33 \text{at} 298\,K, S = 0$$

The total alkalinity (TA) [159] is defined as the sum of all bases, minus the acids present, i.e.

$$TA = [HCO_3-] + 2[CO_3{}^2-] + [B(OH)_4-] + [OH^-] + [HPO_4{}^2-] + 2[PO_4{}^3-] + [HSiO_4-] + [NH_3] + [HS^-] - [H^+] - [HSO_4-] - [HF] - [H_3PO_4]$$

Carbonate alkalinity (A_C) is defined as: $A_C = [HCO_3-] + 2[CO_32-] + [OH^-] - [H^+]$ and can be used to estimate TA in seawater (≈2.4 mM) by correcting for conservative species such as $[B(OH)_4{}^-]$.

The alkalinity is responsible for the buffering of natural waters [158] and its measurement is critical in understanding the environmental impacts of increasing carbon dioxide concentrations in the oceans.

The carbonate system can be quantitatively described by the use any two of the system parameters, Ac, H+, DIC, p_{CO_2}, [HCO_3-] or [CO_32-] from which all of the others can be derived [159].

Of these parameters, field determination of DIC and p_{CO_2} is favoured because this obviates the necessity for separate pH, alkalinity or individual carbonate species measurements.

6.3.1. T_{CO_2} (DIC) and p_{CO_2}

T_{CO_2}, the total dissolved inorganic carbon concentration, can be readily determined by gas diffusion (GD) FIA after acidification of the sample, e.g. by injection into an acidic carrier, or conversely by injection of acid into a continuously flowing sample stream, followed by detection of the carbon dioxide that diffuses through the gas diffusion membrane. Similarly, p_{CO_2}, the "free carbon dioxide" is measured by passing unaltered sample across the membrane and detecting the CO_2 that migrates into the acceptor stream. The diffused carbon dioxide is most commonly detected by spectrophotometric measurement of the change in absorbance of a pH indicator in a weakly buffered acceptor [160], or by monitoring changes in the electrical conductivity of the acceptor stream [161,162]. Other detection systems reported for sensing diffused carbon dioxide include a tungsten oxide sensor [163] chemiluminescence [164], and a bulk acoustic wave detector [165].

Recent examples of the use of GD-FIA to inorganic C speciation in marine water include the work of Pencharee et al. [166] who used a contactless capacitively coupled conductivity detector (C4D) with a deionised water acceptor stream to determine DIC in estuarine waters. Similarly, Martinotti et al. [167] have described a dual GD-FIA system for the determination of both DIC and free CO_2 using conventional conductimetric detection which was effectively used for the determination of both parameters in fresh and marine waters. Faber et al. have also reported a GD-FIA probe system that used spectrophotometric detection for the determination of p_{CO_2} in sediments and overlying waters [168].

6.3.2. Total alkalinity

Total alkalinity determinations of marine waters have classically been performed by an acid–base Gran titration [169]. Flow analysis versions of this approach have been reported using flow through potentiometric detection [170,171] or spectrophotometric detection using the peak width quantification method [172]. An alternative approach involves the on-line acidification of the sample to ca. pH 4 with a buffer, followed by spectrophotometric detection of the released CO_2 that passes through a GD membrane (see Table 3) [173]. Whilst this approach detects only the carbonate alkalinity, suitable correction can be made for other conservative alkalinity species based on the salinity of the sample.

6.3.3. Total and dissolved organic carbon

The determination of these parameters requires removal of inorganic carbon prior to conversion of organic carbon to carbon dioxide which is then detected by techniques such as non-dispersive IR, spectrophotometry or conductimetry, as outlined above for the determination of DIC and CO_2. The conversion process may involve wet oxidation, high temperature catalytic oxidation (HTCO) or photo-oxidation, and is performed on either whole sample (total organic carbon, TOC), or the membrane filtered fraction (dissolved organic carbon, DOC). The methodology of DOC determination in marine samples has been somewhat contentious, and historically the HTCO method has been favoured [174]. However, SCFA methods utilising wet oxidation have been shown to be effective for seawater analysis when appropriate quality assurance protocols are applied [175]. Photo-oxidation has also been used in SCFA [176], FIA [177] and SIA [178] for complete oxidation followed by photometric detection of the released CO_2 that passed through a gas diffusion into an indicator acceptor stream. However chloride in seawater is oxidized to chlorine during photo-oxidation, and this also diffuses through the GD membrane, interfering in the photometric detection. Whilst this effect may be overcome by the addition of hydroxylamine to the indicator stream [176], or by the use of conductimetric detection, there has been little application of FIA/SIA to seawater DOC analysis. Santos et al. recently described a SIA system for the determination of DIC, free dissolved carbon dioxide (CO_2), TC, DOC and alkalinity in inland waters [179]. With minor modification, e.g. for chloride interference in TC and DOC, such multi-parameter SIA systems show considerable promise for comprehensive underway determinations of carbon species in marine waters.

6.4. Silicon

Silicon occurs in natural waters mainly as reactive silica, i.e., soluble SiO_2^- and as short chain polymers, but also as longer polymers and the inorganic and organic fractions of suspended material. Silicon can be a limiting element for phytoplankton growth, and reactive silica is probably the only form that is readily available for diatom growth [155]. Silicon is conventionally determined by spectrophotometric detection of silico-molybdenum blue, using a similar chromogenic reaction to that used for phosphate, and the determination has been performed using FIA [180,181], most recently using LWCC cells for high sensitivity measurements [44,182].

7. Micronutrients

7.1. Iron

Iron (Fe) is the fourth most abundant element in the Earth's crust (~5.6%) [183] but dissolved Fe concentrations in open-ocean waters are often sub-nanomolar [184]. Furthermore, the marine biogeochemistry of Fe is complicated by its redox speciation, low solubility and involvement in biological cycles. Robust methods for the quantification of iron fractions, e.g., labile, dissolved, colloidal, organically bound, particulate, are therefore essential to enhance our understanding of Fe biogeochemistry. The major sources of Fe to the world's oceans are atmospheric, fluvial, hydrothermal, continental shelf regeneration and upwelling of Fe-enriched subsurface waters. In remote areas, the main oceanic source of Fe is from atmospheric dust deposition and in surface waters biological processes are the main Fe removal pathway.

Iron plays an important role in ocean biogeochemistry, being a key micronutrient that regulates marine productivity in large areas of the world oceans such as high-nutrient, low-chlorophyll (HNLC) regions of the world's oceans, which has important implications for global carbon cycling [184]. Such hypotheses have been tested in the under-productive waters of the equatorial Pacific [185], sub-arctic North Pacific [186] and Southern Ocean [186], in which seeding surface ocean water with low concentrations of dissolved Fe triggered a massive phytoplankton bloom and resulted in a significant drawdown of surface water nitrate and atmosphere CO_2. Conceptual and numerical models of ocean biogeochemistry must therefore include Fe as a limiting component [187], and the accuracy of such models will only be improved by routinely including Fe analysis alongside the major nutrients during modern-day oceanographic field campaigns. An interesting paradox in the ocean is that whilst planktonic microorganisms mediate the chemistry and cycling of Fe, the element exerts an influence on the growth

of organisms and the cycling of other nutrients such as carbon and nitrogen.

There are two different types of detection system used in flow injection analysis of Fe; chemiluminescence (CL) and spectrophotometry (SP) (Table 4). Regardless of the method used, preconcentration of Fe onto a chelating resin is necessary to both concentrate and separate the Fe from bulk seawater matrix. The majority of FIA techniques utilise 8-hydroxyquinoline (8-HQ) as the functional chelating group immobilized on a chemically-resistant vinyl polymer resin (e.g., Toyopearl TSK), as developed by Landing et al. [188]. More recent studies have used commercially available chelating resins such as NTA 'Superflow' [189] and Toyopearl AF-Chelate-650 [190], thereby eliminating the synthesis step involved in using 8-HQ. Due to the speciation of Fe, a key consideration is the pH dependency on the recovery of Fe(III) and Fe(II) on the preconcentration column. For example, Fe(III) is recovered by 8-HQ at pH 3.0–4.2, whilst at pH 5.2–6.0 both Fe(III) and Fe(II) are quantitatively recovered [191]. Therefore, flow injection analysis may also allow the redox speciation of dissolved Fe to be determined by careful choice of the pretreatment pH, reagent conditions and appreciation of possible interferences [26,192]. For "total" dissolved Fe(II + III) analysis, either an oxidation step (addition of 10 μM hydrogen peroxide (H_2O_2); [189]) or a reduction step (addition of 100 μM sodium sulphite; [63]) is required prior to preconcentration.

FIA-CL methods are based on the catalytic effect of either Fe(II) or Fe(III) ions on the oxidation of luminol (5-amino-2,3-dihydro-1,4-phthalazinedione) to generate blue luminescence (λ_{max} ~440 nm) which is detected using a photomultiplier tube (PMT). There are two basic FIA-CL approaches. FIA-CL[FeII] methods (e.g. [63]) determine Fe(II) and require acidified samples to be reduced off-line using sodium sulphite. Reduced samples are buffered in-line using NH_4Ac to pH 5 prior to preconcentration on an 8-HQ resin. Fe(II) ions are eluted from the resin using 0.09 M HCl and mixed with a luminol/carbonate buffer reagent stream. Bowie et al. achieved a detection limit of 40 pM, the RSD (n = 5) was ±3.2% for a 1 nM Fe sample [63]. A typical FIA-CL analytical manifold is shown in Fig. 9.

FIA-CL [FeIII] methods (e.g., [191]) determine Fe(III) and also total dissolved Fe if acidified samples are first oxidised off-line using H_2O_2. The acidified, oxidised samples are buffered in-line with NH_4Ac to pH 3 prior to preconcentration. Fe(III) ions are eluted from the resin using 0.3 M HCl. An additional 2 m heated coil is required in the manifold to efficiently mix the eluted Fe(III) with a luminol/carbonate buffer reagent stream and a H_2O_2 stream (which serves as the oxidant for the luminol reaction) before detection at the PMT. The average blank for this method has been reported as 32 ± 14 pM Fe (n = 19) with a detection limit of 5.7 ± 2.9 pM.Fe (n = 4) [193]. To validate the accuracy of trace metal determinations using FIA-CL (and all other methods) it is recommend that a suitable "consensus value" reference seawater sample such as SAFe (sampling and analysis of Fe) is analysed. Acidified SAFe surface and SAFe deep (1000 m) samples from the North Pacific have been widely used by the oceanographic community. Klunder et al. [193] obtained a mean ± SD value of 0.11 ± 0.012 nM (n = 7) for the surface sample and 0.96 ± 0.06 nM (n = 10) for the deep sample which are in excellent agreement with SAFe consensus value of 0.097 ± 0.007 nM and 0.91 ± 0.17 nM from the surface and deep water samples respectively.

FIA-SP involves the catalytic oxidation of DPD (N,N-dimethyl-p-phenylenediamine dihydrochloride) by Fe(III) cycled with H_2O_2 [189,194]. The catalytic nature of the reaction increases the sensitivity of this method, as the amount of oxidised DPD is proportional to the concentration of Fe. H_2O_2 (10 μM) should be added to the sample to ensure oxidation to Fe(III). Depending on the resin used for preconcentration, the samples may need to be buffered in-line. Fe is eluted from the resin and mixes with DPD/buffer and H_2O_2, producing coloured semiquinone derivatives, which are detected spectrophotometrically at 514 nm. The average blank for this method was 60 ± 8 pM Fe (n = 35) with a detection limit of 24 ± 4.9 pM Fe (n = 9) [189]. SAFe surface samples gave a mean ± SD value of 0.10 ± 0.009 nM (n = 14) and SAFe deep 0.93 ± 0.04 nM (n = 18) which are in excellent agreement with SAFe consensus value of 0.097 ± 0.007 nM and 0.91 ± 0.17 nM from surface and deep respectively [189].

7.2. Cobalt

Cobalt (Co) is an essential micronutrient for aquatic organisms as it is required for the synthesis of vitamin B_{12} and is a cofactor in the enzyme carbonic anhydrase [195] and is required by the abundant marine cyanobacteria *Prochlorococcus* and *Synechococcus* [196]. Recent studies have shown that Co may limit or co-limit algal growth in some oceanic regions [197,198]. Oceanic Co concentrations are extremely low, 4–100 pM in surface waters [199,200], and Co has a similar distribution to Fe in the ocean which is strongly influenced by biological uptake, recycling, scavenging and remineralistion. Cobalt is reported to be complexed by organic ligands [196,201] but to a lesser extent than Fe. For example, Noble et al. reported that >75% of Co was organically complexed in South Atlantic waters [202].

Hirata et al. reported an FIA-CL method for the determination of dissolved Co(II) in sea water based on preconcentration using 8-quinolinol immobilised on silica gel, fluoride containing metal alkoxide glass (8HQ-MAF) and CL detection with gallic acid-hydrogen peroxide [203]. Cobalt was eluted with dilute hydrochloric acid and mixed with the reagent solutions at 60 °C. The detection limit was 0.62 ng L^{-1}, the RSD (n = 10) was ± 2.1% for 10 ng L^{-1} cobalt and throughput was 7 h^{-1}. The replacement of gallic acid with pyrogallol enhanced the sensitivity [204], with the pyrogallol–hydrogen peroxide–sodium hydroxide reaction taking place in the presence of methanol (as an activator) and the surfactant cetyltrimethylammonium bromide (CTAB). The practical limit of detection in coastal seawater was 5 pM. This method was adapted for shipboard use in open ocean environments by Shelley et al. [205], with a detection limit of 4.5 pM. The key modifications were: (1) use of a commercially available iminodiacetate (IDA) resin (Toyopearl AF-chelate 650 M) in place of 8-hydroxyquinoline for online preconcentration and matrix removal, (2) use of acidified ammonium acetate (pH 4) as a column-conditioning step before sample loading and rinsing and, most importantly, (3) UV irradiation of acidified seawater samples to determine total dissolved cobalt, rather than an operationally defined fraction. This manifold is shown in Fig. 10 in both the load (Fig. 10a) and the inject (Fig. 10b) configurations and a typical spatial distribution profile for Co using this method is shown in Fig. 10c.

Acidified North Pacific deep seawater (1000 m) samples from the SAFe programme gave a mean ± SD value of 40.9 ± 2.6 pM (n = 9), in excellent agreement with the SAFe consensus value of 43 ± 4 pM, and the result for NASS-5 was 208 ± 30 pM compared with the certified value 187 ± 51 pM.

An FIA method with spectrophotometric detection has also been reported, based on the catalytic effect of Co(II) on the oxidation of N,N′-diethyl-*p*-phenylenediamine by hydrogen peroxide in the presence of Tiron as an activator [206]. The catalytic activity was significantly enhanced by the presence of sea-water matrix components, especially calcium ions. The comparatively weak basic medium (pH 8.7–9.0) of the reaction and its relative freedom from co-existing ions allowed direct analysis of seawater. The limit of detection, as quoted in the original paper, was 1 ng L^{-1}, the RSD was 2–8% (n = 5) for 10–100 ng L^{-1} and the sampling rate was 50 h^{-1}.

Table 4
Summary of selected flow analysis techniques used for micronutrient determinations in marine and estuarine waters.

Parameter	Technique	Basis of method	Analytical performance	Notes	Ref.
Iron					
Fe(II + III) Fe(III) reduction using sulphite. Preconcentrated on 8-hydroxyquinoline (8-HQ). Luminol chemiluminescence detection.	FIA-CL	Samples acidified to pH 2.0. Mapped dissolvable Fe(II + III) concentrations along the Atlantic Meridional Transect from 50°N to 50°S.	LOD (3 s): 40 pM with 1.5 mL sample Repeatability: 3.2% RSD (1.0 nM Fe sample ($n = 5$)). Throughput: One analytical cycle in 3 min		[63]
Fe(II + III)	FIA-SP	Samples acidified to pH 1.7. Preconcentrated on nitrilotriacetic acid (NTA). Catalytic spectrophotometric detection with N,N-dimethyl-p-phenylenediamine dihydrochloride.		Tested with SAFe surface (S) water and SAFe deep (D2).	[189]
Fe(II)	FIA-CL	Luminol chemiluminescence detection.	LOD (3 s): 8–12 pM. Repeatability: RSD 0.9–7.6% ($n = 4$) over the range 8–1000 pM L^{-1}.	Used for day-night deployment during a north-to-south transect of the Atlantic Ocean and a daytime transect in the Sub-Antarctic Front.	[26]
Fe(III)	FIA-CL	Samples acidified. Preconcentrated on 8-HQ. Luminol chemiluminescence detection.	LOD: 0.05 nM with 18 mL sample.	Applied to oceanic waters and hydrothermal waters collected in the North and South Pacific Oceans.	[191]
Fe(III)	FIA-CL	Samples acidified to pH 1.8. Preconcentrated on iminodiacetic acid (IDA) resin. Luminol chemiluminescence detection.	LOD (3 s): 5.7 ± 2.9 pM.	Tested with SAFe surface (S) water and SAFe deep (D2) water. Measured vertical profiles along a 1° latitudinal section at the Zero meridian.	[193]
Fe(III)	FIA-SP	Samples acidified with 1 mL 6 M HCl L^{-1}. Preconcentrated on 8-HQ. Catalytic spectrophotometric detection with N,N-dimethyl-p-phenylenediamine dihydrochloride.	LOD: 0.025 nM. Repeatability: RSD 2.5% ($n = 6$) for 0.35 nM Fe.	Applied to open ocean water samples from the equatorial Pacific and the North Atlantic and hydrothermal plume samples from around Loihi Seamount in the Central Pacific.	[194]
Cobalt					
Co(II)	FIA-CL	Preconcentrated on 8-HQ immobilized on silica gel, fluoride containing metal alkoxide glass (8HQ-MAF). Chemiluminescence detection with gallic acid-hydrogen peroxide. Heated to 60 °C.	LOD (3 s): 0.62 ng L^{-1}. Throughput: The analysis time including the 2-min sample load was 8 min per sea water sample.	Tested with NASS and CASS.	[203]
Co(II)	FIA-CL	Chemiluminescence detection based on the pyrogallol-hydrogen peroxide-sodium hydroxide reaction in the presence of methanol and the surfactant cetyltrimethylammonium bromide (CTAB).	LOD (3 s): 5 pM. Repeatability: RSDs 2.1–5.8% ($n = 3$). Linear range: 5–850 pM.	Tested with NASS-5 CASS-3 and SLEW-2. Applied to samples from the Irish Sea and Tamar Estuary (UK).	[204]
Co(II)	FIA-CL	Samples acidified to 0.024 M and UV irradiated. Preconcentrated on commercially available iminodiacetate (IDA) resin (Toyopearl AF-chelate 650 M). Chemiluminescence detection based on the pyrogallol-hydrogen peroxide-sodium hydroxide reaction in the presence of methanol and the surfactant cetyl trimethylammonium bromide (CTAB).	LOD (3 s): 4.5 pM. Repeatability: RSD ≤4% ($n = 9$). Linear range: 3.8–2000 pM.	Tested with SAFe deep (D2) water and NASS-5. Applied to vertical profile samples from the Sargasso Sea.	[205]

Table 4 (*Continued*)

Parameter	Technique	Basis of method	Analytical performance	Notes	Ref.
Co(II)	FIA-SP	Samples acidified to pH 2. Catalytic effect of Co(II) on the oxidation of N,N′-diethyl-p-phenylenediamine by hydrogen peroxide in the presence of Tiron as an activator.	LOD: 1 ng L^{-1}. Repeatability: RSD 2–8% ($n = 5$). for 10–100 ng L^{-1} Co(II). Throughput: 50 h^{-1}.	Tested with CASS-2 and NASS-2.	[206]
Copper					
Cu(II)	FIA-CL	Samples drawn directly into the manifold via PTFE tubing. Preconcentrated on 8-HQ. Detection based on formation of a Cu-1,10-phenanthroline complex and subsequent oxidation by hydrogen peroxide.	LOD: 0.4 nM. Throughput: 8 min $sample^{-1}$. Standard additions method.	Tested with CASS-1 and NASS-1. Applied to a vertical profile from a near shore station off Pt. Piedras Blancas, California.	[68]
Cu(II)	FIA-CL	Samples acidified to pH 2. Reaction of copper with 1,10-phenanthroline.	LOD: 0.1 nM. Standard additions method.	Used to measure copper complexation throughout the water column in Monterey Bay, California.	[214]
Cu(II)		Samples filtered and UV irradiated with H_2O_2. Preconcentrated on 8-HQ. Detection based on formation of a Cu-1,10-phenanthroline complex and subsequent oxidation by hydrogen peroxide.	Calibration standards in the range 10^{-6} to 10^{-7} M.	Tested with NASS-4 and SLEW-2. Applied to samples from the Celtic Sea and Tamar Estuary (UK). Focused on sample irradiation.	[209]
Zinc					
Zn(II)	FIA-FL	Preconcentrated on 8-HQ. The organic indicator ligand, p-tosyl-8-aminoquinoline, was used to form a complex with zinc.	LOD (3 s): 0.1 nM for a 4.4 mL sample.	Tested with CASS-2 and NASS-2.	[52]
Zn(II)	FIA-FL	Preconcentrated on 8-HQ. The organic indicator ligand, p-tosyl-8-aminoquinoline, was used to form a complex with Zn.	LOD (3 s): 0.06 nM. Repeatability: SD 0.018 nM ($n = 5$). Linear range: 0–4 nM.	Tested with SAFe surface (S1) water. Applied on 2009 CLIVAR 15 cruise across the southern Indian Ocean (from Cape Town, South Africa to Fremantle, Australia).	[219]
Zn(II)	SI-FL	Unacidified seawater matrix. The organic reagent FluoZin-3 was used to form a complex with Zn.	LOD: 0.3 nM. Repeatability: RSD < 2.5%. Linear range: up to 40 nM. Throughput: An analytical cycle of ~1 min per sample.	Used subtropical South Pacific Ocean seawater.	[51]
Manganese					
	FIA-CL	Preconcentrated on 8-HQ. Mn(II) catalysed the oxidation of 7,7,8,8-tetracyanoquinodimethane in an alkaline solution.	LOD (3 s): 0.1 nM. Repeatability: RSD typically 3% for 1–10 nM. Throughput: 6 min per sample. Standard additions method.	Tested with CASS-1 and NASS-1. Applied to a depth profile to 2000 m at a station off the California coastline.	[66]
	FIA-CL	Electrolytic preconcentration using a glassy carbon electrode. Chemiluminescence detection with luminol.		Applied to seawater samples collected in seas adjacent to Japan.	[251]

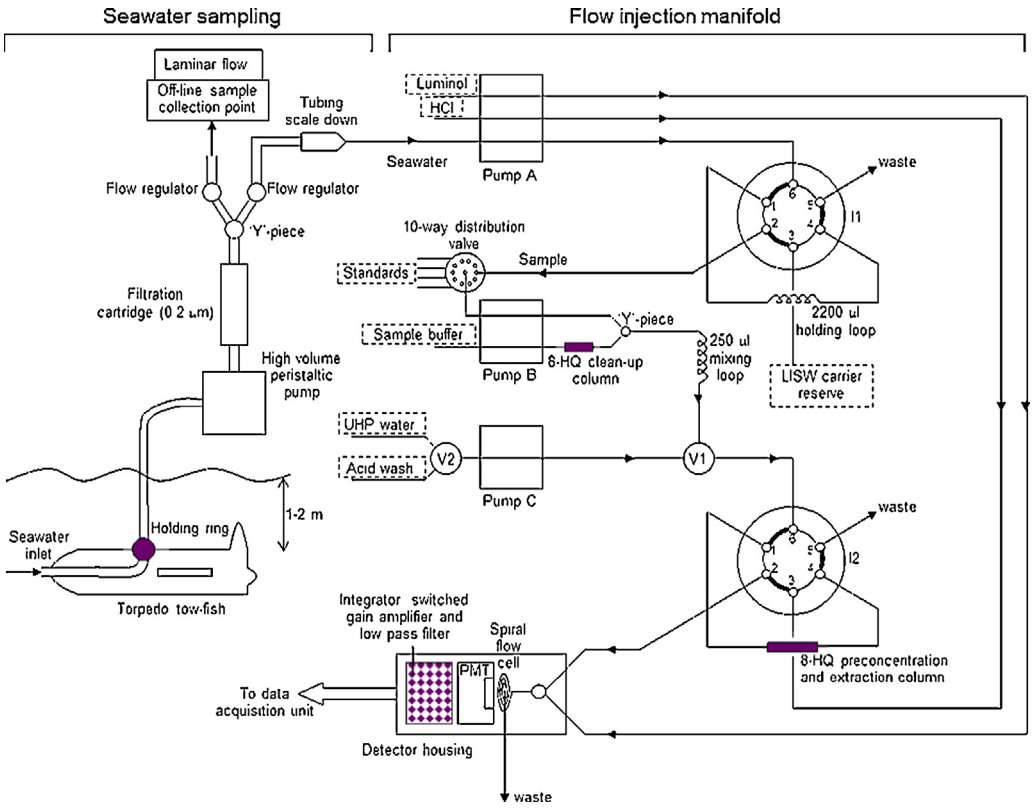

Fig. 9. Schematic of the flow system used for the on-line determination of iron(II) in surface seawater. The left-hand side shows the in situ torpedo fish, high volume pumping and filtration system, whilst the right-hand side shows the components and tubing within the FIA manifold. Pump A delivers a continuous stream of surface seawater and CL reagents, pump B delivers sample solution and sample buffer and pump C delivers UHP water and acid wash solutions. Seawater from the LISW carrier reserve is not preconcentrated onto the 8HQ column and is simply used to prevent air entering the holding loop when sample solution is drawn up by pump B. The holding loop consists of 5 m of 0.75 mm i.d. PTFE tubing. V1 and V2 are solenoid switching valves, I1 and I2 are 6-port, 2-way injection valves. Boxes shown as dotted lines indicate the solution is sealed from the atmosphere within double zip-lock bags. Reproduced with permission from "A.R. Bowie, E.P. Achterberg, P.N. Sedwick, S. Ussher, P.J. Worsfold, Environ. Sci. Technol, 36 (2002) 4600" [26]. Copyright 2002 American Chemical Society.

7.3. Copper

Copper (Cu) is an essential micronutrient involved in enzyme reactions and photosynthetic electron transport processes. At enhanced concentrations however dissolved Cu(II) can be toxic to marine biota. It can inhibit the growth of dinoflagellates at concentrations $<10^{-13}$ M, resulting in decreased fecundity and even death [207]. Natural riverine, aeolian and hydrothermal venting inputs and anthropogenic inputs from e.g. mine waste, sewage effluent and antifouling paints, can elevate Cu concentrations in marine waters, particularly in coastal ecosystems. Open ocean dissolved Cu concentrations are typically in the range 0.5–6 nM, with >98% in the organically complexed form [208,209]. These organic ligands are classified as either weak ($K'_{CuL} = 10^{7}$–10^{11}), usually restricted to the upper water column, or strong ($K'_{CuL} = 10^{12}$–10^{15}), usually found throughout the water column [210]. Recent studies have shown that Cu plays a critical role in the physiology of open ocean phytoplankton as under conditions of Fe limitation, marine phytoplankton up regulate a high affinity Fe transport system which utilities Cu containing oxidases [211,212]. The redox state of dissolved Cu (Cu(I) versus Cu(II)) may control the uptake of Cu, rather than the concentration of the inorganic species in solution [213].

There have been few shipboard FIA methods for the determination of Cu, predominantly based on FIA-CL. Coale et al. reported the first of these in 1992, based on the formation of a complex between copper and 1,10-phenanthroline and the subsequent emission of light during oxidation of the complex by hydrogen peroxide [68]. Preconcentration and matrix removal were achieved with an in-line 8-hydroxyquinoline column. The detection limit was 0.4 nM with a 4 mL sample volume and a throughput of 7 h^{-1}. A refinement of the method gave a lower detection limit of 0.1 nM without preconcentration [214] and the method was used to measure copper complexation throughout the water column in Monterey Bay, California. Two ligand classes were identified: a strong ligand (L1; $\log K'_1$ 13.1 ± 0.4), ranging from 1.3 to 3.1 nM, and a weaker ligand (L2; $\log K'_2$ 9.4 ± 0.6), ranging from 9.4 to 25.6 nM. Achterberg et al. [209] compared off-line (4 h, 400 W + peroxide) with in-line (quartz coil, volume 2.8 mL + peroxide) UV digestion in combination with in-line preconcentration and phenanthroline FIA-CL detection for the determination of total dissolved copper. They showed that UV digestion was necessary to determine total dissolved Cu, as was the case for Co, and that recoveries were higher with the off-line method.

7.4. Zinc

Surface ocean zinc (Zn) concentrations are low and may limit photosynthetic activity in many oceanic regimes which, in turn, may impact on global carbon cycling. This is because Zn plays an important role in the metabolism of marine phytoplankton by acting as an essential constituent of enzymes linked with carbon [215] and phosphate uptake [216]. Dissolved Zn concentrations profiles resemble those of the major nutrients, with large deep to surface concentration ratios [217,218]. Concentrations of dissolved Zn are <0.1 nM in surface waters of the world's oceans [217–219], with approximately 98% of this pool chelated by strong organic ligands [220,221]. This reduces the bioavailable fraction of Zn, the free metal ion, to concentrations as low as 1 pM, values which have

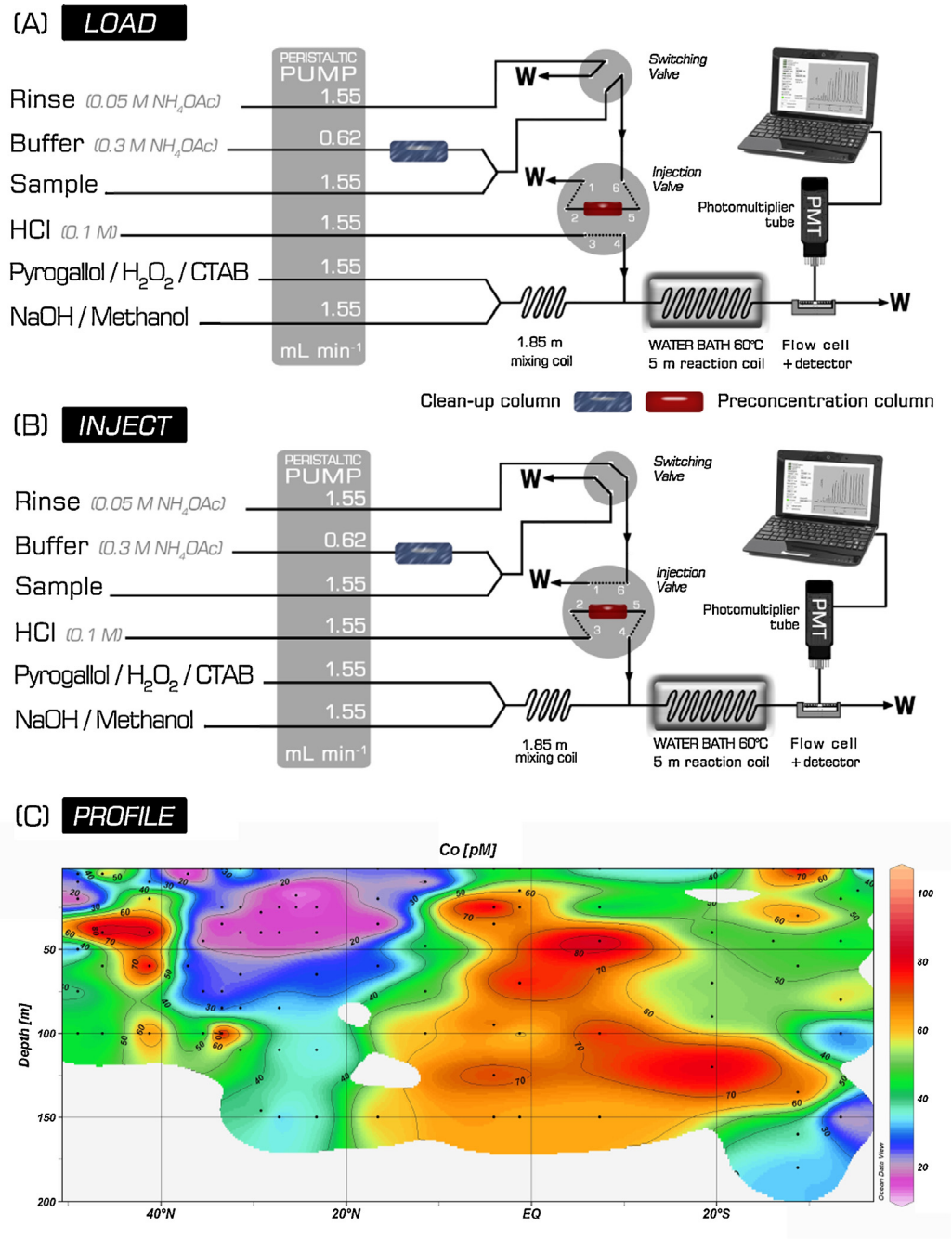

Fig. 10. Manifold configuration for the determination of total dissolved cobalt in seawater. (A) shows the manifold in the sample load position and (B) shows the manifold in the inject position. (C) shows the ocean scale spatial mapping of Co on a north-south transect of the Atlantic Ocean using FIA-CL detection.

been shown to limit phytoplankton growth in culture experiments [222–225]. Culture experiments have revealed that at low dissolved Zn concentrations, the ability of phytoplankton to manufacture carbonic anhydrase is diminished, potentially limiting CO_2 uptake and growth [215,226]. However, at present there is a lack of dissolved Zn data for most regions of the world's oceans, partly due to a lack of suitable shipboard analytical methods. Zinc is a notoriously pervasive contaminant, as it is frequently used on marine vessels and equipment. Therefore accurate measurements can only be made using strict safeguards during sample collection and analysis [219,221].

Nowicki et al. reported a sensitive FIA method for the shipboard determination of Zn with fluorimetric detection in 1994 [52]. A cation exchange column was used for preconcentration and the separation of Zn from interfering alkali and alkaline earth ions. The ligand, *p*-tosyl-8-aminoquinoline (pTAQ), selectively complexed zinc to give a fluorescent product with a detection limit of 0.1 nM for a 4.4 mL sample and a precision of ±6% ($n = 5$) for a 4.3 nM Zn standard. A depth profile of 12 samples plus standards and blanks was analysed in triplicate in 5.5 h. This method was recently adapted for shipboard use for low level Zn concentrations in the Indian Ocean [219]. The key modifications were: (1) using 40 μM of pTAQ and (2) use of 0.16 M ammonium acetate buffer (pH 5.7) as the rinse step. The detection limit was 0.06 ± 0.018 nM ($n = 5$). The accuracy of the method was demonstrated using SAFe surface where 0.06 nM was obtained which is within the consensus values of 0.062 ± 0.019 nM [219]. As cadmium (Cd) also forms a fluorescence complex with pTAQ this can result in a

positive inference with this method. Cadmium is present at much lower concentrations approximately 10% of Zn in seawater [220]. Nowicki et al. [52] reported that Cd fluorescence is approximately 30% of the Zn signal which would result in about a 3% correction. Gosnell et al. [219] did not correct for Cd in their work as the calculated Cd interference was below their detection limit.

More recently, Grand et al. designed and optimised a sequential injection lab-on-valve system with fluorescence detection, using the selective reagent FluoZin-3, for the determination of zinc in unacidified seawater [51]. Optimum response was obtained with a large sample volume (75 μL) aspirated last in the sequence prior to flow reversal and detection, giving a detection limit of 0.3 nM, RSDs <2.5%, a linear range of 0.3–40 nM and a throughput of 60 h^{-1}. The method was suitable for shipboard deployment, did not require a preconcentration/matrix removal step and was suitable for the determination of zinc in open ocean waters.

7.5. Manganese

Manganese (Mn) is a biogeochemical reactive element, and is found in the oceans at concentrations ranging from <0.1 to 25 nM [227] and generally low concentrations in the range of 0.1–0.2 nM in the surface ocean [228]. Dissolved Mn is an essential trace nutrient, which is used in enzymes for various biological processes such as photosystem II (PSII) for the splitting of water in phytoplankton to supply electrons to the reaction system of PSII [229]. Manganese is also essential in superoxide dismutase (SOD) enzymes in marine diatoms [230]. Manganese(II) is removed from the dissolved phase oxidation to insoluble manganese(IV) oxide, which acts as a scavenger for other trace elements. Particulate Mn(IV) in sediments is diffused into the water column under mild reducing conditions, such as the oxygen minimum layer and near-shore anoxic sediments. Sources of manganese to the oceans include aeolian dust, coastal, sediment release, riverine and hydrothermal inputs. Manganese is an excellent tracer of a wide variety of marine biogeochemical process, such as Fe input from continental margins and hydrothermal vents [231,232] and aeolian inputs [233].

Analogous to Fe, there are two types of detection system used for the FIA determination of Mn, chemiluminescence (CL) and spectrophotometry (SP). FIA-CL methods are based on the catalytic effect of Mn ions on the oxidation of 7,7,8,8-tetracyanoquinodimethane (TCNQ) or luminol [66,234]. Chapin, Johnson and Coale [66] presented a FIA-CL method based on the Mn(II)-catalysis of the oxidation of 7,7,8,8-tetracyanoquinodimethane (TCNQ) in alkaline solution. By incorporating a mini-column containing the 8-HQ chelating resin, a limit of detection of 0.1 nM was achieved. This method has been widely used at sea where profiles were in good agreement with data measured by GF-AAS in a shore-based laboratory. The reaction was also exploited by Bowie et al. [235] in order to determine manganese in potable waters. No chelating resin mini-column was incorporated into the FIA system since the nature of the matrix and the enhanced Mn levels meant the reaction was sensitive enough without in-line preconcentration. Bowie et al. [235] investigated the reaction mechanism in detail and the CL emission was sensitised using eosin Y and further enhanced by means of didodecyldimethylammonium bromide (DDAB) bilayer vesicles.

More recently, Doi et al. [234] used the catalytic effect of Mn ions on the oxidation of luminol and hydrogen peroxide to develop a highly sensitive method for the determination of picomolar concentrations of Mn. Seawater samples were buffered to pH 8.5 with ammonium acetate and reconcentrated onto an 8-HQ chelating resin. The Mn was eluted from the column with dilute HCl, mixed with ammonium hydroxide and luminol solution and passed through a 3 m mixing coil at 25 °C. This FIA-CL method was recently used by Middag et al. [232] where they changed the buffer to ammonium borate and buffered the samples in-line. The blank, determined by measuring column-cleaned seawater over a Toyopearl AF-Chelate 650 M resin and an 8-HQ column, was 0.02 nM with a detection limit of <0.01 nM and a RSD of 2.19% ($n = 22$). Analysis of SAFe surface and SAFe deep samples were 0.73 ± 0.01 nM and 0.31 ± 0.01 nM ($n = 3$) respectively. These values are within the consensus range of 0.74 ± 0.06 nM and 0.35 ± 0.06 nM.

FIA-SP involves the catalytic oxidation of either N,N-diethylaniline or leucomalachite green by periodate and manganese [236,237]. Kolotyrkina et al. reported a shipboard method combining in-line preconcentration on an ion-exchange microcolumn with spectrophotometric detection based on the catalytic effect of Mn(II) on the oxidation of N,N-diethylaniline by potassium periodate at neutral pH. The linear range was 0.01–20 μg L^{-1} (0.2–364 nM) with a sampling frequency of 15 h^{-1} and the method was applied to the measurement of manganese in deep sea samples as a tracer for active hydrothermal vents [238]. A more sensitive method FIA-SP for determining Mn at low oceanic concentrations by pre-concentrating Mn on 8-HQ resin at pH 8.5 and involved the catalytic oxidation of malachite green by periodate and manganese was reported by Resing and Mottl [237]. Aguilar-Islas et al. [239] added nitrilotriacetic acid as an activator ligand to this FIA-SP method, which increased the reaction rate and resulted in better sensitivity, and use a commercially available Toyopearl resin for pre-concentration. Mn is eluted from the resin and mixes with periodate/buffer and sodium periodate producing malachite green that is detected spectrophotometrically at 620 nm. The average blank for this method was 0.07 ± 0.01 nM ($n = 4$) with a detection limit of 0.03 nM [239]. The accuracy of the method was tested using NASS-4 (National Research Council, Canada) certified reference material, with concentrations of 6.7 ± 0.2 nM determined, which was within 3% of the certified value of 6.9 ± 0.4 nM [239].

8. Emerging trends

Flow and sequential injection systems offer a number of definite advantages for the analysis of marine waters. They are compact, use little reagent and/or sample, show excellent repeatability, and because they are closed systems, enable trace analyses to be performed under conditions that minimise the potential for contamination. Furthermore, complex sample manipulations (e.g. filtration, digestion, derivatization, preconcentration) are readily performed and automated using a flow/sequential injection system, making them an ideal platform for underway shipboard or in situ monitoring applications, e.g. in tethered buoys, as described by Répécaud et al. [240]. There has been limited, but continuing development of FIA in submersible systems and on remotely operated vehicles (ROVs) [128–131,180,241–246], and there is great potential in this area, given the developments in microfluidic devices during the last decade. The microfluidic flow device described by Beaton et al. for the determination of nitrate [247] is an example of the new generation of flow analysis devices under development. The emergence of new reagentless sensors, such as that recently described for silicate [248] will also greatly facilitate the development of in situ flow systems.

Flow injection analysis offers a powerful means of efficiently manipulating samples on-line, with procedures such sample matrix modification, e.g. NaCl removal [249] and digestion [34] becoming more common. Improvements in method detection limits are anticipated as increasing use is made of high-sensitivity detectors such as LWCCs coupled with miniature solid state spectrometers and as more innovative applications of chemiluminescence are developed. Whilst this review focuses on methodologies suitable for shipboard use, it should also be stressed that flow injection coupled with ICP-MS combines the attractive features of both for the laboratory based

determination of micronutrient species, particularly in conjunction with on-line solid phase preconcentration and matrix removal.

Better understanding of the biogeochemistry of the oceans is inextricably related to the quality and comprehensiveness of available analytical data. Flow injection analysis and related techniques have a continuing and important role to play in the acquisition of this information.

Acknowledgements

RC acknowledges funding by the EMRP via JRP-ENV05-REG1 (Metrology for ocean salinity and acidity) and GF acknowledges funding by the EMRP via JRP-ENV05 (Metrology for ocean salinity and acidity). The EMRP is jointly funded by the EMRP participating countries within EURAMET and the European Union. The authors thank Dr. Angela Milne (Plymouth University) for providing some of the Co data for the data quality case study.

References

[1] R. Costanza, Ecol. Econ. 31 (1999) 199.
[2] R. Costanza, R. d'Arge, R. de Groot, S. Farber, M. Grasso, B. Hannon, S. Naeem, K. Limberg, J. Paruelo, R.V. O'Neill, R. Raskin, P. Sutton, M. van der Belt, Nature 387 (1997) 253.
[3] V.N. de Jonge, M. Elliott, Hydrobiologia 475/476 (2002) 1.
[4] V.N. de Jonge, M. Elliott, in: J. Steele, S. Thorpe, K. Turekian (Eds.), Encyclopedia of Marine Sciences, Academic Press, London, 2001, p. 3399.
[5] R.S. Arthurton, H.H. Kremer, E. Odada, W. Salomons, J.I. Marshall Crossland, African Basins: LOICZ Global Change Assessment and Synthesis of River Catchment-Coastal Sea Interaction and Human Dimensions, LOICZ, Texel, The Netherlands, 2002, pp. 344.
[6] L.D. de Lacerda, H.H. Kremer, B. Kjerfve, W. Salomons, J.I. Marshall Crossland, C.J. Marshall Crossland, South American Basins: LOICZ Global Change Assessment and Synthesis of River Catchment-Coastal Sea Interaction and Human Dimensions, LOICZ, Texel, The Netherlands, 2002, pp. 212.
[7] G.H. Hong, H.H. Kremer, J. Pacyna, C.-T.A. Chen, H. Behrendt, W. Salomons, J.I. Marshall Crossland, East Asia Basins: LOICZ Global Change Assessment and Synthesis of River Catchment-Coastal Sea Interaction and Human Dimensions, LOICZ, Texel, The Netherlands, 2002, pp. 262.
[8] B. Kjerfve, W.J. Wiebe, H.H. Kremer, W. Salomons, W. Salomons, J.I.C. Marshall Crossland, N. Morcom, N. Harvey, J.I. Marshall Crossland, Caribbean Basins:, LOICZ Global Change Assessment and Synthesis of River Catchment/Island-Coastal Sea Interaction and Human Dimensions; With A Desktop Study of Oceania Basins, LOICZ, Texel, The Netherlands, 2002, pp. 127.
[9] S.B. Bricker, J.G. Ferreira, T. Simas, Ecol. Modell. 169 (2003) 39.
[10] R.K. Turner, W.N. Adger, I. Lorenzoni, Towards Integrated Modelling and Analysis in Coastal Zones: Principles and Practices, LOICZ, Texel, The Netherlands, 1998, pp. 122.
[11] P.J. Statham, Sci. Tot. Environ. 434 (2012) 213.
[12] D. Karl, The Biological Pump and the Ocean Carbon Cycle, American Society of Limnology and Oceanography Ocean Fertilization Symposium, American Society of Limnology and Oceanography, Washington, DC, 2001.
[13] R.C. Schenck, Mar. Biol. Lett. 5 (1984) 13.
[14] M. Gledhill, K.N. Buck, Front. Micriobiol. 3 (2012) 1.
[15] B.A. Bergquist, E.A. Boyle, Global Biogeochem. Cycles 20 (2006) GB1015.
[16] K.S. Johnson, R.M. Gordon, K.H. Coale, Mar. Chem. 57 (1997) 137.
[17] London Convention, London Convention and Protocol: Convention on the Prevention of Marine Pollution by Dumping of Wastes and Other Matter 1972 and 1996 Protocol, www.imo.org/OurWork/Environment/SpecialProgrammesAndInitiatives/Pages/London-Convention-and-Protocol.aspx (accessed 19.10.12).
[18] Helsinki Convention, Convention on the Protection of the Marine Environment of the Baltic Sea Area, 1992 (entered into force on 17 January 2000), www.helcom.fi/Convention/en_GB/text/ (accessed 19.12.12).
[19] Barcelona Convention, Convention for the Protection of The Mediterranean Sea Against Pollution, www.unep.ch/regionalseas/regions/med/t_barcel.htm (accessed 19.10.12).
[20] European Commission, Off. J. Eur. Commun. L206 (1992) 7.
[21] European Commission, Off. J. Eur. Union L164 (2008) 19.
[22] I.D. McKelvie, in: S.D. Kolev, I.D. McKelvie (Eds.), Advances in Flow Injection Analysis and Related Techniques, Elsevier, Amsterdam, 2008.
[23] P.J. Worsfold, I.D. McKelvie, G. Hanrahan, in: S.D. Kolev, I.D. McKelvie (Eds.), Advances in Flow Injection Analysis and Related Techniques, Elsevier, Amsterdam, 2008, p. 685.
[24] E.A.G. Zagatto, C.C. Oliveira, A. Townshend, P.J. Worsfold, Flow Analysis with Spectrophotometric and Luminometric Detection, Elsevier, Amsterdam, 2012.
[25] W. Petersen, M. Petschatnikov, F. Schroeder, F. Colijn, in: H. Dahlin, N.C. Flemming, K. Nittis, S.E. Petersson (Eds.), Building the European Capacity in Operational Oceanography. Proceedings of the Third International Conference on EuroGOOS. Elsevier Oceanography Series, Elsevier, 2003, p. 325.
[26] A.R. Bowie, E.P. Achterberg, P.N. Sedwick, S. Ussher, P.J. Worsfold, Environ. Sci. Technol. 36 (2002) 4600.
[27] P.C.F.C. Gardolinski, A.R.J. David, P.J. Worsfold, Talanta 58 (2002) 1015.
[28] S.M. Gray, G. Hanrahan, I.D. McKelvie, A. Tappin, F. Tse, P.J. Worsfold, Environ. Chem. 3 (2006) 3.
[29] C.H. Lueck, D.F. Boltz, Anal. Chem. 28 (1956) 1168.
[30] S. Motomizu, T. Wakimoto, K. Toei, Analyst 108 (1983) 361.
[31] P.S. Ellis, A.J. Lyddy-Meaney, P.J. Worsfold, I.D. McKelvie, Anal. Chim. Acta 499 (2003) 81.
[32] S.K. Mishra, P.K. Dasgupta, Anal. Chim. Acta 605 (2007) 166.
[33] P.S. Ellis, A.M. Haji Shabani, B. Gentle, I.D. McKelvie, Talanta 84 (2011) 98.
[34] B.S. Gentle, P.S. Ellis, P.A. Faber, M.R. Grace, I.D. McKelvie, Anal. Chim. Acta 674 (2010) 117.
[35] B.S. Gentle, P.S. Ellis, M.R. Grace, I.D. McKelvie, Anal. Chim. Acta 704 (2011) 116.
[36] J. Hodge, B. Longstaff, A. Steven, P. Thornton, P. Ellis, I. McKelvie, Mar. Pollut. Bull. 51 (2005) 113.
[37] A.J. Lyddy-Meaney, P. Ellis, P.J. Worsfold, E.C.V. Butler, I.D. McKelvie, Talanta 58 (2002) 1043.
[38] R.B.R. Mesquita, M.T.S.O.B. Ferreira, I.V. Tóth, A.A. Bordalo, I.D. McKelvie, A.O.S.S. Rangel, Anal. Chim. Acta 701 (2011) 15.
[39] L.J. Gimbert, P.J. Worsfold, TrAC 26 (2007) 914.
[40] W. Frenzel, I.D. McKelvie, in: S.D. Kolev, I.D. McKelvie (Eds.), Advances in Flow Injection Analysis and Related Techniques, Elsevier, Amsterdam, 2008, p. 311.
[41] L.J. Gimbert, P.M. Haygarth, P.J. Worsfold, Talanta 71 (2007) 1624.
[42] Q.P. Li, D.A. Hansell, J.Z. Zhang, Limnol. Oceanogr. Methods 6 (2008) 319.
[43] J. Ma, D. Yuan, M. Zhang, Y. Liang, Talanta 78 (2009) 315.
[44] J. Ma, R.H. Byrne, Talanta 88 (2012) 484.
[45] A. Sanz-Medel, J.M. Costa-Fernandez, in: P. Worsfold, A. Townshend, C. Poole (Eds.), Encyclopedia of Analytical Science, second edition, Elsevier, Oxford, 2005, p. 149.
[46] M.E. Diaz-Garcia, R. Badia-Laino, in: P. Worsfold, A. Townshend, C. Poole (Eds.), Encyclopedia of Analytical Science, second edition, Elsevier, Oxford, 2005, p. 97.
[47] E.A.G. Zagatto, C.u.C. Oliveira, A. Townshend, P.J. Worsfold, Flow Analysis with Spectrophotometric and Luminometric Detection, Elsevier, Amsterdam, 2012, pp. 95.
[48] S. Motomizu, M. Oshima, N. Katsumura, Anal. Sci. Technol. 8 (1995) 843.
[49] R.T. Masserini Jr., K.A. Fanning, Mar. Chem. 68 (2000) 323.
[50] R.J. Watson, E.C.V. Butler, L.A. Clementson, K.M. Berry, J. Environ. Monit. 7 (2005) 37.
[51] M. Grand, H.M. Oliveira, J. Ruzicka, C. Measures, Analyst 136 (2011) 2747.
[52] J.L. Nowicki, K.S. Johnson, K.H. Coale, V.A. Elrod, S.H. Lieberman, Anal. Chem. 66 (1994) 2732.
[53] A.K. Campbell, Chemiluminescence: Principles and Applications in Biology and Medicine, Ellis Horwood, Chichester, 1988.
[54] A.R. Bowie, M.G. Sanders, P.J. Worsfold, Lumin. Chemilumin. 11 (1996) 61.
[55] K. Robards, P.J. Worsfold, Anal. Chim. Acta 266 (1992) 147.
[56] A.R. Bowie, E.P. Achterberg, S. Ussher, P.J. Worsfold, J. Autom. Methods Manage. (2005) 37.
[57] P.J. Worsfold, E.P. Achterberg, A.R. Bowie, V. Cannizzaro, S. Charles, J.M. Costa, F. Dubois, R. Pereiro, B. San Vicente, A. Sanz-Medel, R. Vandeloise, E. Vander Donckt, P. Wollast, S. Yunus, J. Autom. Methods Manage. Chem. 24 (2002) 41.
[58] D. Price, P.J. Worsfold, R.F.C. Montoura, Anal. Chim. Acta 298 (1994) 121.
[59] J. Yuan, A.M. Shiller, Anal. Chem. 71 (1999) 1975.
[60] L.L. Klopf, T.A. Nieman, Anal. Chem. 55 (1983) 1080.
[61] R.A. Nickson, S.J. Hill, P.J. Worsfold, Anal. Proc. 32 (1995) 387.
[62] W.M. Landing, C. Haraldsson, N. Paxeus, Anal. Chem. 58 (1986) 3031.
[63] A.R. Bowie, E.P. Achterberg, R.F.C. Mantoura, P.J. Worsfold, Anal. Chim. Acta 361 (1998) 189.
[64] V.A. Elrod, K.S. Johnson, K.H. Coale, Anal. Chem. 63 (1991) 893.
[65] R.T. Powell, D.W. King, W.M. Landing, Mar. Chem. 50 (1995) 13.
[66] T.P. Chapin, K.S. Johnson, K.H. Coale, Anal. Chim. Acta 249 (1991) 469.
[67] C.M. Sakamoto-Arnold, K.S. Johnson, Anal. Chem. 59 (1987) 1789.
[68] K.H. Coale, K.S. Johnson, P.M. Stout, C.M. Sakamoto, Anal. Chim. Acta 266 (1992) 345.
[69] M.C. Yebra, N. Carro, M.F. Enriquez, A. Moreno-Cid, A. Garcia, Analyst 126 (2001) 933.
[70] M. Del Carmen Yebra, L. Rodriguez, L. Puig, A. Moreno-Cid, Microchim. Acta 140 (2002) 219.
[71] T. Seki, Y. Hirano, K. Oguma, Anal. Sci. 18 (2002) 351.
[72] A. Yuzefovsky, R.F. Lonardo, M. Wang, R.G. Michel, J. Anal. At. Spectrom. 9 (1994) 1195.
[73] Y. Liang, D. Yuan, Q. Li, Q. Lin, Mar. Chem. 103 (2007) 122.
[74] A.C.B. Dias, E.P. Borges, E.A.G. Zagatto, P.J. Worsfold, Talanta 68 (2006) 1076.
[75] I.D. McKelvie, D.M.W. Peat, G.P. Matthews, P.J. Worsfold, Anal. Chim. Acta 351 (1997) 265.
[76] S. Auflitsch, D.M.W. Peat, I.D. McKelvie, P.J. Worsfold, Analyst 122 (1997) 1477.
[77] F.R.P. Rocha, J.A. Nobrega, J. Braz. Chem. Soc. 8 (1997) 625.
[78] T. Yamane, J. Flow Inj. Anal. 12 (1995) 176.
[79] E.A.G. Zagatto, M.A.Z. Arruda, A.O. Jacintho, I.L. Mattos, Anal. Chim. Acta 234 (1990) 153.
[80] S. Jambunathan, P.K. Dasgupta, D.K. Wolcott, G.D. Marshall, D.C. Olson, Talanta 50 (1999) 481.

[81] H. Liu, P.K. Dasgupta, Anal. Chim. Acta 289 (1994) 347.
[82] ISO/IEC, General requirements for the competence of testing and calibration laboratories, ISO/IEC 17025:2005, International Organization for Standardization/International Electrotechnical Commission, Geneva, 2005.
[83] W.M. Landing, G.A. Cutter, J.A. Dalziel, A.R. Flegal, R.T. Powell, D. Schmidt, A. Shiller, P. Statham, S. Westerlund, J. Resing, Mar. Chem. 49 (1995) 253.
[84] J.M. Bewers, J. Dalziel, P.A. Yeats, J.L. Barron, Mar. Chem. 10 (1981) 173.
[85] A.R. Bowie, E.P. Achterberg, S. Blain, M. Boye, P.L. Croot, H.J.W. de Baar, P. Laan, G. Sarthou, P.J. Worsfold, Mar. Chem. 84 (2003) 19.
[86] A.R. Bowie, E.P. Achterberg, P.L. Croot, H.J.W. De Baar, P. Laan, J.W. Moffett, S. Ussher, P.J. Worsfold, Mar. Chem. 98 (2006) 81.
[87] S.J. Ussher, I. Petrov, C.R. Quetel, P.J. Worsfold, Environ. Chem. 7 (2010) 139.
[88] M. Aoyama, C. Anstey, J. Barwell-Clarke, F. Baurand, S. Becker, M. Blum, S.C. Coverly, E. Czobik, F. d'Amico, I. Dahllof, M. Dai, J. Dobson, O. Pierre-Duplessix, M. Duval, C. Engelke, G.-C. Gong, O. Grosso, A. Hirayama, H. Inoue, Y. Ishida, D.J. Hydes, H. Kasai, R. Kerouel, M. Knockaert, N. Kress, K.A. Krogslund, M. Kumagai, S.C. Leterme, C. Mahaffey, H. Mitsuda, P. Morin, T. Moutin, D. Munaron, A. Murata, G. Nausch, H. Ogawa, J. van Ooijen, J. Pan, G. Paradis, C. Payne, G. Prove, P. Raimbault, M. Rose, K. Saito, H. Saito, K. Sato, C. Schmidt, M. Schutt, T.M. Shammon, S. Olafsdottir, J. Sun, T. Tanhua, S. Weigelt-Krenz, L. White, E.M.S. Woodward, P.J. Worsfold, T. Yoshimura, A. Youenou, J.-Z. Zhang, in: S. Yoshikawa (Ed.), Technical Reports of the Meteorological Research Institute No. 60: 2008 Inter-laboratory Comparison Study of a Reference Material for Nutrients in Seawater, Meteorological Research Institute Japan, 2008, p. 138.
[89] M. Aoyama, H. Ota, M. Kimura, T. Kitao, H. Mitsuda, A. Murata, K. Sato, Anal. Sci. 28 (2012) 911.
[90] D.J. Hydes, M. Aoyama, A. Aminot, K. Bakker, S. Becker, S. Coverly, A. Daniel, A.G. Dickson, O. Grosso, R. Kerouel, J. van Ooijen, K. Sato, T. Tanhua, E.M.S. Woodward, J.Z. Zhang, Recommendations for the Determination of Nutrients in Seawater to High Levels of Precision and Inter-Comparability using Continuous Flow Analysers http://www.go-ship.org/Manual/Hydes_et_al_Nutrients.pdf, http://www.go-ship.org/Manual/Hydes_et_al_Nutrients.pdf (accessed 19.03.13).
[91] GEOTRACES Standards and Intercalibration Committee, Sampling and Sample Handling protocols for GEOTRACES Cruises, http://www.geotraces.org/libraries/documents/Intercalibration/Cookbook.pdf (accessed 19.03.13).
[92] JCGM, International Vocabulary of Basic and General Terms in Metrology, Paris, 2008, p. 108.
[93] M.H. Ramsey, J. Anal. At. Spectrom. 13 (1998) 97.
[94] V.J. Barwick, S.L.R. Ellison, B. Fairman, Anal. Chim. Acta 394 (1999) 281.
[95] JCGM, Evaluation of measurement data — guide to the expression of uncertainty in measurement (GUM), Paris, 2008, p. 120.
[96] S.L.R. Ellison, W.A. (Eds.), Eurachem/CITAC Guide: Quantifying Uncertainty in Analytical Measurement, Eurachem, 2012.
[97] S.L.R. Ellison, V.J. Barwick, Analyst 123 (1998) 1387.
[98] V.J. Barwick, Preparation of Calibration Curves: A Guide to Best Practice, LGC, Teddington, 2003.
[99] J. Kragten, Analyst 119 (1994) 2161.
[100] R. Brix, S.H. Hansen, V. Barwick, J. Tjornelund, Analyst 127 (2002) 140.
[101] I.D. McKelvie, D.M.W. Peat, P.J. Worsfold, Anal. Proc. 32 (1995) 437.
[102] P. Monbet, I.D. McKelvie, in: L.M.L. Nollet (Ed.), Handbook of Water Analysis, CRC Press, New York, Basel, 2007, p. 219.
[103] I.D. McKelvie, A.J. Lyddy-Meaney, in: P.J. Worsfold, A. Townshend, C. Poole (Eds.), Encyclopedia of Analytical Science, Elsevier Science, 2005, p. P167.
[104] K.S. Johnson, R.L. Petty, Anal. Chem. 54 (1982) 1185.
[105] C. Frank, F. Schroeder, R. Ebinghaus, W. Ruck, Talanta 70 (2006) 513.
[106] Y. Udnan, I.D. McKelvie, M.R. Grace, J. Jakmunee, K. Grudpan, Talanta 66 (2005) 461.
[107] J.M. Gasol, A.J.M. Zehnder, Sci. Mar. 61 (1997) 213.
[108] G. Nürnberg, Water Res. 18 (1984) 369.
[109] M. Grace, Y. Udnan, I. McKelvie, J. Jakmunee, K. Grudpan, Environ. Chem. 3 (2006) 19.
[110] T.H. Fang, Estuar. Coastal Shelf Sci. 50 (2000) 689.
[111] M. Suzumura, E.D. Ingall, Mar. Chem. 75 (2001) 141.
[112] P.C.F.C. Gardolinski, P.J. Worsfold, I.D. McKelvie, Water Res. 38 (2004) 688.
[113] C.R. Benitez-Nelson, L. O'Neill, L.C. Kolowith, P. Pellechia, R. Thunell, Limnol. Oceanogr. 49 (2004) 1593.
[114] J.M. Estela, V. Cerdá, Talanta 66 (2005) 307.
[115] I.D. McKelvie, B.T. Hart, T.J. Cardwell, R.W. Cattrall, Analyst 114 (1989) 1459.
[116] O. Tue-Ngeun, P. Ellis, I.D. McKelvie, P. Worsfold, J. Jakmunee, K. Grudpan, Talanta 66 (2005) 453.
[117] R.L. Benson, I.D. McKelvie, B.T. Hart, Y.B. Truong, I.C. Hamilton, Anal. Chim. Acta 326 (1996) 29.
[118] D.M.W. Peat, I.D. McKelvie, G.P. Mathews, P.M. Haygarth, P.J. Worsfold, Talanta 45 (1997) 47.
[119] R.L. Benson, I.D. McKelvie, B.T. Hart, I.C. Hamilton, Anal. Chim. Acta 291 (1994) 233.
[120] M.I.G.S. Almeida, M.A. Segundo, J.L.F.C. Lima, A.O.S.S. Rangel, Talanta 64 (2004) 1283.
[121] A. Aminot, R. Kerouel, Mar. Chem. 76 (2001) 113.
[122] P.J. Worsfold, P. Monbet, A. Tappin, M. Fitzsimons, D. Stiles, I.D. McKelvie, Anal. Chim. Acta 624 (2008) 37.
[123] J.K. Moore, S.C. Doney, D.M. Glover, I.Y. Fung, Deep Sea Res. Part II 49 (2001) 463.
[124] J.D.H. Strickland, T.R. Parsons, A Practical Handbook of Seawater Analysis, Fisheries Research Board of Canada, Ottawa, 1972.
[125] V.M. Ivanov, J. Anal. Chem. 59 (2004) 1002.
[126] K.S. Johnson, R.L. Petty, Limnol. Oceanogr. 28 (1983) 1260.
[127] C.M. Sakamoto, G.E. Friederich, S.K. Service, F.P. Chavez, Deep Sea Res. Part I 43 (1996) 1763.
[128] A. Daniel, D. Birot, S. Blain, P. Treguer, B. Leilde, E. Menut, Mar. Chem. 51 (1996) 67.
[129] A.R.J. David, T. McCormack, A.W. Morris, P.J. Worsfold, Anal. Chim. Acta 361 (1998) 63.
[130] A.R.J. David, T. McCormack, P.J. Worsfold, J. Autom. Methods Manage. Chem. 21 (1999) 1.
[131] N. Le Bris, P.M. Sarradin, D. Birot, A.M. Alayse-Danet, Mar. Chem. 72 (2000) 1.
[132] APHA-AWWA-WEF, Standard methods for the examination of water and wastewater, centennial edition, Washington, 2005.
[133] C. Gal, W. Frenzel, J. Möller, Microchim. Acta 146 (2004) 155.
[134] F. Nydahl, Talanta 21 (1974) 1259.
[135] B.C. Madsen, Anal. Chim. Acta 124 (1981) 437.
[136] M.T. Oms, A. Cerda, V. Cerda, Anal. Chim. Acta 315 (1995) 321.
[137] P.F. Pratt, K. Nithipatikom, W.B. Campbell, Anal. Biochem. 231 (1995) 383.
[138] I.G. Torro, J.V.G. Mateo, J.M. Calatayud, Anal. Chim. Acta 366 (1998) 241.
[139] P.S. Ellis, Unpublished data.
[140] R. Kérouel, A. Aminot, Mar. Chem. 57 (1997) 265.
[141] C. Pasquini, L. Cardosode Faria, Anal. Chim. Acta 193 (1987) 19.
[142] P.O.J. Hall, R.C. Aller, Limnol. Oceanogr. 37 (1992) 1113.
[143] M. Van Son, R.C. Schothorst, G. Den Boef, Anal. Chim. Acta 153 (1983) 271.
[144] S.W. Willason, K.S. Johnson, Mar. Biol. 91 (1986) 285.
[145] S.M. Gray, P.S. Ellis, M.R. Grace, I.D. McKelvie, Spectrosc. Lett. 39 (2006) 737.
[146] H.A. McKenzie, TrAC 13 (1994) 138.
[147] P.A. Kammerer, M.G. Rodel, R.A. Hughes, G.F. Lee, Environ. Sci. Technol. 1 (1967) 340.
[148] F. Koroleff, in: K. Grasshoff, M. Ehrhardt, K. Kremling (Eds.), Methods of Seawater Analysis, Verlag Chemie, Weinheim, 1976, p. 162.
[149] F.A.J. Armstrong, P.M. Williams, J.D.H. Strickland, Nature 211 (1966) 481.
[150] L. Woo, W. Maher, Anal. Chim. Acta 315 (1995) 123.
[151] I.D. McKelvie, M. Mitri, B.T. Hart, I.C. Hamilton, A.D. Stuart, Anal. Chim. Acta 293 (1994) 155.
[152] A. Cerda, M.T. Oms, R. Forteza, V. Cerda, Anal. Chim. Acta 351 (1997) 273.
[153] M.T. Oms, V. Cerda, A. Cerda, J. Autom. Chem. 18 (1996) 113.
[154] S. Hinkamp, G. Schwedt, Z. Wasser-Abwasser-Forsch. 24 (1991) 60.
[155] K. Robards, I.D. McKelvie, R.L. Benson, P.J. Worsfold, N.J. Blundell, H. Casey, Anal. Chim. Acta 287 (1994) 147.
[156] C.L. Sabine, R.A. Feely, N. Gruber, R.M. Key, K. Lee, J.L. Bullister, R. Wanninkhof, C.S. Wong, D.W.R. Wallace, B. Tilbrook, F.J. Millero, T.-H. Peng, A. Kozyr, T. Ono, A.F. Rios, Science 305 (2004) 367.
[157] The Royal Society, Ocean Acidification Due to Increasing Atmospheric Carbon Dioxide Contents, The Royal Society, London, 2005, pp. 68.
[158] W. Stumm, J.J. Morgan, Aquatic Chemistry, John Wiley and Sons, Inc., NY, 1996.
[159] R.E. Zeebe, D. Wolf-Gladrow, CO_2 in Seawater: Equilibrium, Kinetics, Isotopes, Elsevier, New York, 2001.
[160] S. Motomizu, K. Toei, T. Kuwaki, M. Oshima, Anal. Chem. 59 (1987) 2930.
[161] T. Aoki, Y. Fujimaru, Y. Oka, K. Fujie, Anal. Chim. Acta 284 (1993) 167.
[162] V. Kubán, P.K. Dasgupta, Talanta 40 (1993) 831.
[163] L. Monser, N. Adhoum, S. Sadok, Talanta 62 (2004) 389.
[164] T. Aoki, K. Ito, M. Munemori, Anal. Lett. 21 (1988) 1881.
[165] S.Z. Yao, X.L. Su, J. AOAC Int. 82 (1999) 1479.
[166] S. Pencharee, P.A. Faber, P.S. Ellis, P. Cook, J. Intaraprasert, K. Grudpan, I.D. McKelvie, Anal. Methods 4 (2012) 1278.
[167] V. Martinotti, M. Balordi, G. Ciceri, Anal. Bioanal. Chem. 403 (2012) 1083.
[168] P.A. Faber, I.D. McKelvie, P. Cook, P.S. Ellis, Anal. Chim. Acta 691 (2011) 1.
[169] A.G. Dickson, Deep Sea Res. Part A 28 (1981) 609.
[170] D.R. Turner, S. Knox, M. Whitfield, C. dos Santos, Anal. Proc. 24 (1987) 360.
[171] A. Watanabe, H. Kayanne, K. Nozaki, K. Kato, A. Negishi, S. Kudo, H. Kimoto, M. Tsuda, A.G. Dickson, Mar. Chem. 85 (2004) 75.
[172] R.B.R. Mesquita, A.O.S.S. Rangel, Anal. Sci. 20 (2004) 1205.
[173] S. Gray, M.R. Grace, P.S. Ellis, I.D. McKelvie, Talanta 77 (2008) 533.
[174] G. Spyres, M. Nimmo, P.J. Worsfold, E.P. Achterberg, A.E.J. Miller, TrAC 19 (2000) 498.
[175] A. Aminot, R. Kerouel, Analusis 18 (1990) 289.
[176] W. Schreurs, Hydrolog. Bull. 12 (1978) 137.
[177] R.T. Edwards, I.D. McKelvie, P. Ferrett, B.T. Hart, J.B. Bapat, K. Koshy, Anal. Chim. Acta 261 (1992) 287.
[178] O. Tue-Ngeun, R.C. Sandford, J. Jakmunee, K. Grudpan, I.D. McKelvie, P.J. Worsfold, Anal. Chim. Acta 554 (2005) 17.
[179] I.C. Santos, R.B.R. Mesquita, A. Machado, A.A. Bordalo, A.O.S.S. Rangel, Anal. Chim. Acta 778 (2013) 38.
[180] J. Floch, S. Blain, D. Birot, P. Treguer, Anal. Chim. Acta 377 (1998) 157.
[181] J. Thomsen, K.S. Johnson, R.L. Petty, Anal. Chem. 55 (1983) 2378.
[182] N. Amornthammarong, J.Z. Zhang, Talanta 79 (2009) 621.
[183] S.R. Taylor, Geochim. Cosmochim. Acta 28 (1964) 1273.
[184] J.H. Martin, S.E. Fitzwater, Nature 331 (1988) 341.
[185] K.H. Coale, K.S. Johnson, S.E. Fitzwater, R.M. Gordon, S. Tanner, F.P. Chavez, L. Ferioli, C. Sakamoto, P. Rogers, F. Millero, P. Steinberg, P. Nightingale, D. Cooper, W.P. Cochlan, M.R. Landry, J. Constantinou, G. Rollwagen, A. Trasvina, R. Kudela, Nature 383 (1996) 495.

[186] P.W. Boyd, R. Strzepek, S. Takeda, G. Jackson, C.S. Wong, R.M. McKay, C. Law, H. Kiyosawa, H. Saito, N. Sherry, K. Johnson, J. Gower, N. Ramaiah, Limnol. Oceanogr. 50 (2005) 1872.
[187] J.K. Moore, S.C. Doney, Global Biogeochem. Cycles 21 (2007).
[188] W.M. Landing, C. Haraldsson, N. Paxeus, Anal. Chem. 58 (1986) 3031.
[189] M.C. Lohan, A.M. Aguilar-Islas, K.W. Bruland, Limnol. Oceanogr. Methods 4 (2006) 164.
[190] M.P. Hurst, K.W. Bruland, Mar. Chem. 103 (2007) 211.
[191] H. Obata, H. Karatani, E. Nakayama, Anal. Chem. 65 (1993) 1524.
[192] B.M. Hopkinson, K.A. Barbeau, Mar. Chem. 106 (2007) 2.
[193] M.B. Klunder, P. Laan, R. Middag, H.J.W. De Baar, J.C. van Ooijen, Deep Sea Res. Part II 58 (2011) 2678.
[194] C.I. Measures, J. Yuan, J.A. Resing, Mar. Chem. 50 (1995) 3.
[195] T.W. Lane, F.M.M. Morel, Plant Physiol. 123 (2000) 345.
[196] M.A. Saito, J.W. Moffett, S.W. Chisholm, J.B. Waterbury, Limnol. Oceanogr. 47 (2002) 1629.
[197] E.M. Bertrand, M.A. Saito, J.M. Rose, C.R. Riesselman, M.C. Lohan, A.E. Noble, P.A. Lee, G.R. DiTullio, Limnol. Oceanogr. 52 (2007) 1079.
[198] M.A. Saito, T.J. Goepfert, Limnol. Oceanogr. 53 (2008) 266.
[199] M.A. Saito, J.W. Moffett, G.R. DiTullio, Global Biogeochem. Cycles 18 (2004).
[200] R.U. Shelley, P.N. Sedwick, T.S. Bibby, P. Cabedo-Sanz, T.M. Church, R.J. Johnson, A.I. Macey, C.M. Marsay, E.R. Sholkovitz, S.J. Ussher, P.J. Worsfold, M.C. Lohan, Global Biogeochem. Cycles 26 (2012).
[201] J.R. Donat, K.W. Bruland, Anal. Chem. 60 (1988) 240.
[202] A.E. Noble, C.H. Lamborg, D.C. Ohnemus, P.J. Lam, T.J. Goepfert, C.I. Measures, C.H. Frame, K.L. Casciotti, G.R. DiTullio, J. Jennings, M.A. Saito, Limnol. Oceanogr. 57 (2012) 989.
[203] S. Hirata, Y. Hashimoto, M. Aihara, G. Vitharana Mallika, Fresenius. J. Anal. Chem. 355 (1996) 676.
[204] V. Cannizzaro, A.R. Bowie, A. Sax, E.P. Achterberg, P.J. Worsfold, Analyst 125 (2000) 51.
[205] R.U. Shelley, B. Zachhuber, P.N. Sedwick, P.J. Worsfold, M.C. Lohan, Limnol. Oceanogr. Methods 8 (2010) 352.
[206] A. Malahoff, I.Y. Kolotyrkina, L.K. Shpigun, Analyst 121 (1996) 1037.
[207] M. Gledhill, M. Nimmo, S.J. Hill, M.T. Brown, J. Phycol. 33 (1997) 2.
[208] K.H. Coale, K.W. Bruland, Limnol. Oceanogr. 33 (1988) 1084.
[209] E.P. Achterberg, C.B. Braungardt, R.C. Sandford, P.J. Worsfold, Anal. Chim. Acta 440 (2001) 27.
[210] J.W. Moffett, R.G. Zika, L.E. Brand, Deep Sea Res. Part A 37 (1990) 27.
[211] M.T. Maldonado, A.E. Allen, J.S. Chong, K. Lin, D. Leus, N. Karpenko, S.L. Harris, Limnol. Oceanogr. 51 (2006) 1729.
[212] G. Peers, S.A. Quesnel, N.M. Price, Limnol. Oceanogr. 50 (2005) 1149.
[213] D.M. Semeniuk, J.T. Cullen, W.K. Johnson, K. Gagnon, T.J. Ruth, M.T. Maldonado, Deep Sea Res, Part I 56 (2009) 1130.
[214] H. Zamzow, K.H. Coale, K.S. Johnson, C.M. Sakamoto, Anal. Chim. Acta 377 (1998) 133.
[215] F.M.M. Morel, J.R. Reinfelder, S.B. Roberts, C.P. Chamberlain, J.G. Lee, D. Yee, Nature 369 (1994) 740.
[216] Y. Shaked, Y. Xu, K. Leblanc, F.M.M. Morel, Limnol. Oceanogr. 51 (2006) 299.
[217] R.W. Jakuba, M.A. Saito, J.W. Moffett, Y. Xu, Global Biogeochem. Cycles 26 (2012).
[218] M.C. Lohan, P.J. Statham, D.W. Crawford, Deep Sea Res. Part II 49 (2002) 5793.
[219] K.J. Gosnell, W.M. Landing, A. Milne, Mar. Chem. 132 (2012) 68.
[220] K.W. Bruland, Limnol. Oceanogr. 34 (1989) 269.
[221] M.J. Ellwood, C.M.G. Van den Berg, Mar. Chem. 68 (2000) 295.
[222] M.A. Anderson, F.M.M. Morel, R.R.L. Guillard, Nature 276 (1978) 70.
[223] L.E. Brand, W.G. Sunda, R.R.L. Guillard, Limnol. Oceanogr. 28 (1983) 1182.
[224] W.G. Sunda, S.A. Huntsman, Limnol. Oceanogr. 37 (1992) 25.
[225] W.G. Sunda, S.A. Huntsman, Limnol. Oceanogr. 40 (1995) 1404.
[226] P.D. Tortell, G.H. Rau, F.M.M. Morel, Limnol. Oceanogr. 45 (2000) 1485.
[227] J.R. Donat, K.W. Bruland, in: B. Salbu, E. Steinners (Eds.), Trace Metals in Natural Waters, 1995, p. 247.
[228] W.M. Landing, K.W. Bruland, Earth Planet. Sci. Lett. 49 (1980) 45.
[229] W.G. Sunda, S.A. Huntsman, G.R. Harvey, Nature 301 (1983) 234.
[230] G. Peers, N.M. Price, Limnol. Oceanogr. 49 (2004) 1774.
[231] M.B. Klunder, P. Laan, R. Middag, H.J.W. de Baar, K. Bakker, J. Geophys. Res. [Oceans] 117 (2012).
[232] R. Middag, H.J.W. de Baar, P. Laan, P.H. Cai, J.C. van Ooijen, Deep Sea Res. Part II 58 (2011) 2661.
[233] A.M. Shiller, Geochim. Cosmochim. Acta 61 (1997) 4321.
[234] T. Doi, H. Obata, M. Maruo, Anal. Bioanal. Chem. 378 (2004) 1288.
[235] A.R. Bowie, P.R. Fielden, R.D. Lowe, R.D. Snook, Analyst 120 (1995) 2119.
[236] I.Y. Kolotyrkina, L.K. Shpigun, Y.A. Zolotov, A. Malahoff, Analyst 120 (1995) 201.
[237] J.A. Resing, M.J. Mottl, Anal. Chem. 64 (1992) 2682.
[238] I.Y. Kolotyrkina, L.K. Shpigun, Y.A. Zolotov, G.I. Tsysin, Analyst 116 (1991) 707.
[239] A.M. Aguilar-Islas, J.A. Resing, K.W. Bruland, Limnol. Oceanogr. Methods 4 (2006) 105.
[240] M. Répécaud, Y. Dégrés, N. Bernard, J.P. Allenou, Y. Aoustin, J.P. Arrondeau, J.F. Bouget, K. Bucas, A. Daniel, J.F. Guillaud, M. Hamon, P. Jégou, A. Laes, D. Le Roux, D. Le Piver, L. Quemener, J.F. Rolin, T. Rudelle, J. Legrand, R. Vuillemin, New instruments to monitor coastal sea water masses according to European Water Framework Directive, Trophimatique project, OCEANS'09 IEEE Bremen: Balancing Technology with Future Needs, Bremen, 2009.
[241] K.S. Johnson, C.L. Beehler, C.M. Sakamoto-Arnold, Anal. Chim. Acta 179 (1986) 245.
[242] H.W. Jannasch, K.S. Johnson, C.M. Sakamoto, Anal. Chem. 66 (1994) 3352.
[243] D. Thouron, R. Vuillemin, X. Philippon, A. Lourenco, C. Provost, A. Cruzado, V. Garcon, Anal. Chem. 75 (2003) 2601.
[244] P.M. Sarradin, N. Le Bris, C. Le Gall, P. Rodier, Talanta 66 (2005) 1131.
[245] R.J.K. Dunn, P.R. Teasdale, J. Warnken, M.A. Jordan, J.M. Arthur, Environ. Pollut. 148 (2007) 213.
[246] R. Vuillemin, D. Le Roux, P. Dorval, K. Bucas, J.P. Sudreau, M. Hamon, C. Le Gall, P.M. Sarradin, Deep-Sea Res. Part I 56 (2009) 1391.
[247] A.D. Beaton, C.L. Cardwell, R.S. Thomas, V.J. Sieben, F.E. Legiret, E.M. Waugh, P.J. Statham, M.C. Mowlem, H. Morgan, Environ. Sci. Technol. 46 (2012) 9548.
[248] W. Giraud, L. Lesven, J. Jońca, C. Barus, M. Gourdal, D. Thouron, V. Garçon, M. Comtat, Talanta 97 (2012) 157.
[249] E. Grygolowicz-Pawlak, M. Sohail, M. Pawlak, B. Neel, A. Shvarev, R. De Marco, E. Bakker, Anal. Chem. 84 (2012) 6158.
[250] Y. Liang, D. Yuan, Q. Li, Q. Lin, Anal. Chim. Acta 571 (2006) 184.
[251] E. Nakayama, K. Isshiki, Y. Sohrin, H. Karatani, Anal. Chem. 61 (1989) 1392.